Whole-Heart High-Resolution Late Gadolinium Enhancement: Techniques and Clinical Applications

Solenn Toupin, PhD,[1,2,3,4] Théo Pezel, MD,[5,6] Aurélien Bustin, PhD,[2,3,4,7] and Hubert Cochet, MD, PhD[2,3,4,8]*

CME

If you wish to receive credit for this activity, please refer to the website: www.wileyhealthlearning.com/JMRI.

In cardiovascular magnetic resonance, late gadolinium enhancement (LGE) has become the cornerstone of myocardial tissue characterization. It is widely used in clinical routine to diagnose and characterize the myocardial tissue in a wide range of ischemic and nonischemic cardiomyopathies. The recent growing interest in imaging left atrial fibrosis has led to the development of novel whole-heart high-resolution late gadolinium enhancement (HR-LGE) techniques. Indeed, conventional LGE is acquired in multiple breath-holds with limited spatial resolution: ~1.4–1.8 mm in plane and 6–8 mm slice thickness, according to the Society for Cardiovascular Magnetic Resonance standardized guidelines. Such large voxel size prevents its use in thin structures such as the atrial or right ventricular walls. Whole-heart 3D HR-LGE images are acquired in free breathing to increase the spatial resolution (up to $1.3 \times 1.3 \times 1.3$ mm^3) and offer a better detection and depiction of focal atrial fibrosis. The downside of this increased resolution is the extended scan time of around 10 min, which hampers the spread of HR-LGE in clinical practice. Initially introduced for atrial fibrosis imaging, HR-LGE interest has evolved to be a tool to detect small scars in the ventricles and guide ablation procedures. Indeed, the detection of scars, nonvisible with conventional LGE, can be crucial in the diagnosis of myocardial infarction with nonobstructed coronary arteries, in the detection of the arrhythmogenic substrate triggering ventricular arrhythmia, and improve the confidence of clinicians in the challenging diagnoses such as the arrhythmogenic right ventricular cardiomyopathy. HR-LGE also offers a precise visualization of left ventricular scar morphology that is particularly useful in planning ablation procedures and guiding them through the fusion of HR-LGE images with electroanatomical mapping systems. In this narrative review, we attempt to summarize the technical particularities of whole-heart HR-LGE acquisition and provide an overview of its clinical applications with a particular focus on the ventricles.
Evidence Level: 2
Technical Efficacy Stage: 2

J. MAGN. RESON. IMAGING 2022;55:967–987.

BACKGROUND

Cardiovascular magnetic resonance (CMR) is the gold standard modality for characterizing myocardial tissue properties. Over the past decades, late gadolinium enhancement (LGE) has established itself as the cornerstone of this characterization. Its ability to detect myocardial fibrosis makes it a powerful tool for the diagnosis of myocardial infarction (MI) as well as a wide range of nonischemic cardiomyopathies that exhibit different patterns of enhancement. More recently, a growing interest in LA fibrosis has arisen with the aim to guide ablation procedures

View this article online at wileyonlinelibrary.com. DOI: 10.1002/jmri.27732

Received Jan 23, 2021, Accepted for publication Apr 14, 2021.

*Address reprint requests to: H.C., Department of Cardiac Imaging, CHU Bordeaux, IHU Liryc – L'Institut de RYthmologie et modélisation Cardiaque, CHU Bordeaux/Université de Bordeaux/Inserm U1045, Avenue de Magellan, 33604 Pessac, France. E-mail: hcochet@wanadoo.fr

From the [1]Siemens Healthcare France, Saint-Denis, France; [2]IHU Liryc, Electrophysiology and Heart Modeling Institute, Fondation Bordeaux Université, Bordeaux, France; [3]Université de Bordeaux, Centre de recherche Cardio-Thoracique de Bordeaux, Bordeaux, France; [4]INSERM, Centre de recherche Cardio-Thoracique de Bordeaux, Bordeaux, France; [5]Division of Cardiology, Johns Hopkins University, Baltimore, Maryland, USA; [6]Department of Cardiology, Lariboisiere Hospital, APHP, University of Paris, Paris, France; [7]Department of Diagnostic and Interventional Radiology, Lausanne University Hospital and University of Lausanne, Lausanne, Switzerland; and [8]Bordeaux University Hospital (CHU), Pessac, France

and to predict the recurrence of atrial fibrillation.[1,2] However, one of the challenges of current LGE techniques is the limited spatial resolution and the resulting partial volume effect. Indeed, the spatial resolution of conventional LGE sequences remains limited by breath-hold durations (<15–20 sec). The Society of Cardiovascular Magnetic Resonance (SCMR) recommends a spatial resolution of ~1.6–1.8 mm in-plane and 6–8 mm slice thickness to assess LGE in the left ventricle (LV).[3] As a comparison, the LA wall is 2–4 mm thick, underlining the need for higher spatial resolution.[4]

To overcome this limitation, novel free-breathing three-dimensional (3D) high-resolution LGE (HR-LGE) sequences have emerged with the ability to detect fibrosis in thin-walled chambers.[1,5] Despite the extended scan time, HR-LGE imaging gained significant momentum with the DECAAF multicentric study (Delayed-Enhancement MRI Determinant of Successful Radiofrequency Catheter Ablation of Atrial Fibrillation), which investigated the association between LA fibrosis and arrhythmia recurrence after ablation. An important feature of HR-LGE is the whole-heart coverage that offers the ability to reconstruct any desirable views. As clinicians examined these new images, it appeared HR-LGE was also valuable in the right ventricle (RV) and the LV to detect small scars otherwise that were invisible with conventional LGE due to partial volume effect.

This narrative review gives insights into the established methodology of the HR-LGE sequence with its technical particularities as compared with conventional LGE. We highlight the clinical value of using HR-LGE in other chambers than LA, after shortly summarizing actual clinical implications of LA fibrosis imaging. Finally, we describe the latest HR-LGE developments made to bring this technique closer to widespread clinical use.

LATE GADOLINIUM ENHANCEMENT IN CLINICAL ROUTINE

The Principle of LGE

LGE techniques rely on the intravenous injection of a gadolinium-based contrast agent that is distributed in the extracellular space of the myocardium.[6] The gadolinium rapidly washes out of normal tissues, while it is retained in pathological tissues where the extracellular space is increased such as fibrosis, edema, or amyloid deposition. LGE was historically validated on MI, where the extracellular volume is increased in the acute phase with cell membrane ruptures, and in the chronic phase with the cells replaced by collagen. The gadolinium shortens the longitudinal relaxation T1. LGE images are T1-weighted and pathological tissues appear enhanced as compared to healthy myocardium. Recent guidelines recommend to acquire LGE at least 10 min after injection.[3]

Conventional LGE Technique

The clinical standard of LGE is a two-dimensional (2D) multislice acquisition with a typical spatial resolution of ~1.4–1.8 mm in plane, a slice thickness of 6–8 mm, with or without gap, as recommended by the SCMR.[3] Inversion-recovery segmented gradient-echo is the most widely used sequence.[6] The sequence is usually repeated in long-axis (two, three, and four-chamber) and short-axis views. In clinical routine, conventional LGE focuses on the left ventricle due to its limited spatial resolution.

The scan is synchronized to the patient's electrocardiogram (ECG) at end-diastole to minimize cardiac motion. Ideally, the acquisition is performed every other heartbeat (2-RR triggering) to allow for more complete magnetization recovery and thus, a better signal intensity. However, in clinical routine, single heartbeat triggering (1-RR triggering) is sometimes used to save half the scan time.

To avoid image artifacts, the breathing motion is paused using multiple breath-holds per view. A single breath-hold 3D LGE acquisition is also possible with a similar moderate spatial resolution ($1.5 \times 1.5 \times 8\ mm^3$) and longer breath-holds (~20–25 sec with 1-RR triggering) than 2D LGE.[7] This technique ensures a significantly reduced acquisition time compared to 2D with similar image quality and fibrosis quantification.[8–11] One should note that 3D acquisition is not a synonym of high spatial resolution, as the voxel size is similar to that of 2D multislice acquisition.

In LGE imaging, the inversion time is a critical parameter that needs to be tuned for each acquisition. It is set to null the healthy myocardium and ensure the best contrast between healthy and abnormal tissue. A scout sequence is usually performed right before LGE to determine the adequate inversion time (typically 250–300 msec).[6] However, the inversion time increases with gadolinium wash-out and needs to be adjusted accordingly during the CMR exam. Phase-sensitive inversion-recovery (PSIR) is an alternative technique that makes myocardial nulling less sensitive to the precise choice of inversion time.[12] PSIR reconstruction requires the acquisition of a reference image every other heartbeat and is therefore only compatible with 2-RR triggered LGE sequences. This prerequisite makes PSIR impractical with single breath-hold 3D LGE acquisition, as it would double the breath-hold duration to more than 40 sec.

Despite improvement in scar detection with PSIR, the visualization of scars adjacent to the blood pool remains challenging due to a low scar-to-blood contrast. Several approaches for suppressing signal from blood pool have been proposed over the last decade. Magnetization preparation pulses have been inserted before,[13–15] or after[16–19] the inversion recovery pulse, to achieve a simultaneous nulling of the healthy myocardium and the blood pool. If dark-blood LGE improves reader confidence particularly for subendocardial scars compared with conventional LGE,[20] this technique is not widely available on clinical scanners yet. Of note, scar-to-blood contrast can also be improved without additional magnetization preparation by nulling the blood pool instead of the healthy myocardium in conventional LGE with PSIR.[21] However, conventional "bright-blood" LGE remains today the commonly used technique in clinical routine.

The Importance of LGE in Clinical Routine

First, LGE is a crucial diagnostic tool to diagnose various myocardial diseases. Indeed, subendocardial or transmural LGE is characteristic of ischemic heart disease, while subepicardial or midmyocardial LGE suggests nonischemic heart disease.[22] Within nonischemic heart diseases, analysis of the LGE location and distribution can often allow the clinician to distinguish myocarditis, sarcoidosis,[23] hypertrophic or dilated cardiomyopathies,[24] amyloidosis, and others.[25] Second, the analysis of LGE transmurality predicts myocardial viability after MI and is used to select patients who would benefit the most from revascularization. Finally, LGE is a powerful independent prognostic factor for predicting cardiovascular events in both ischemic and nonischemic heart diseases.[26,27]

HIGH-RESOLUTION LATE GADOLINIUM ENHANCEMENT

The HR-LGE sequence is an axial volume that covers the whole heart. The sequence settings are mostly identical for atrial and ventricular HR-LGE, except that 1) the volume positioning that should be centered on the region-of-interest in head-feet direction and 2) the acquisition window should be set to atrial or ventricular diastole, according to the studied chambers.[28]

From Conventional LGE to HR-LGE

As clinicians' interest in atrial LGE imaging increased, the demand for higher spatial resolution increased (Fig. 1). Indeed, for detecting scars in thin-walled atria, smaller voxels became necessary to reduce the partial volume effect. However, increasing the spatial resolution results in noisier images and longer scan times. The lack of signal can be addressed by using 3D rather than 2D acquisition schemes. However, the associated longer scan time makes the acquisition incompatible with breath-holds. Therefore, a free-breathing approach is necessary, with a dedicated strategy to avoid motion artifacts.

Two major free-breathing LGE techniques are currently available in clinical routine: 1) single-shot acquisition combined with in-plane motion compensation and averaging[29,30] and 2) respiratory-gated acquisition.[31,32] The motion-corrected single-shot strategy provides comparable image quality than conventional LGE with similar spatial resolution.

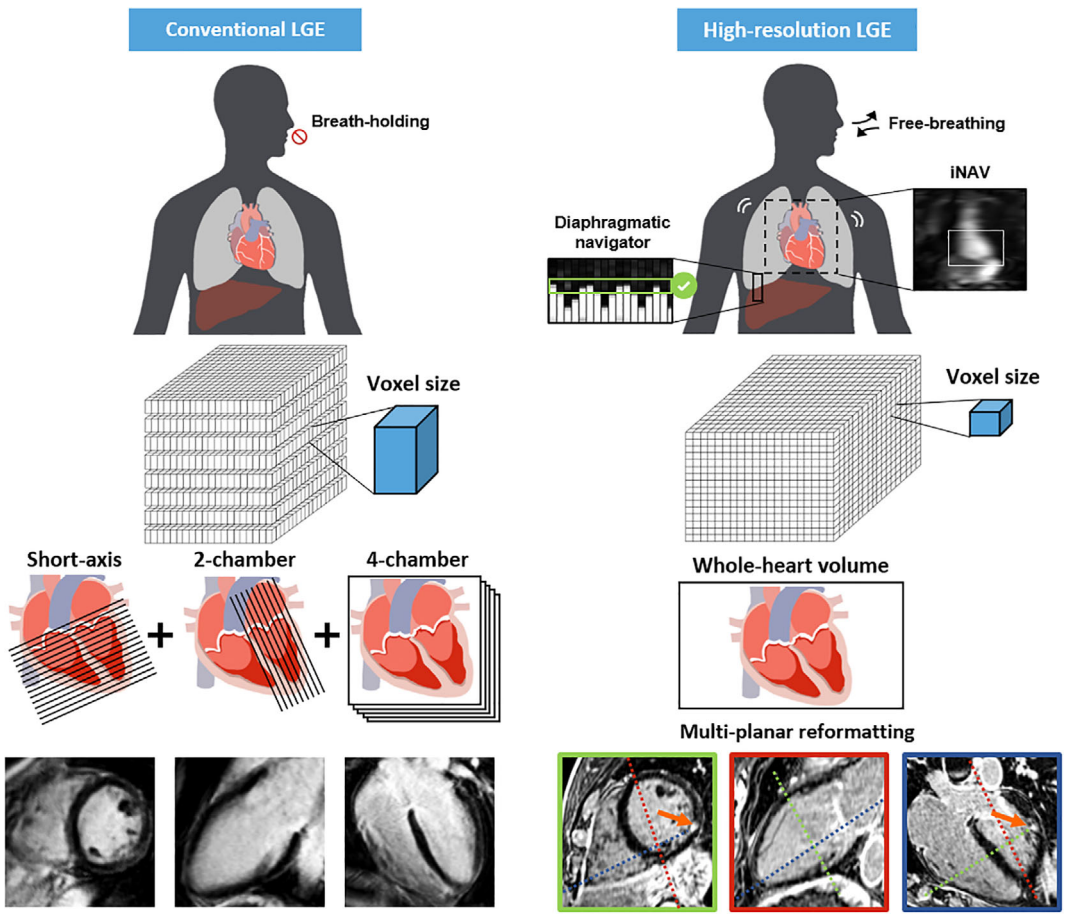

FIGURE 1: Technical differences between conventional and high-resolution LGE acquisitions. Conventional LGE is acquired with several successive breath-holds in short-axis, two- and four-chamber views and a moderate spatial resolution. High-resolution LGE is acquired with free-breathing using an echo-navigator to track the respiratory motion and restrict the acquisition to the expiratory phase. Any desired plane can be reconstructed from the whole-heart volume with multiplanar reformatting.

It is particularly useful in vulnerable patients in whom conventional breath-hold LGE is prone to artifacts.[33,34] However, the single-shot feature of this technique makes it only compatible with 2D imaging and moderate spatial resolution.

On the other hand, the respiratory-gating strategy is compatible with 3D imaging and high spatial resolution which makes it the suitable solution for free-breathing HR-LGE in clinical routine. The breathing motion is tracked in real-time using an echo-navigator made of additional MR pulses.[31,32] This echo-navigator is manually placed on the liver dome to restrict data acquisition to the expiratory phase and reject the rest of the respiratory cycle. The echo-navigator efficiency, which refers to the percentage of respiratory cycle from which data is acquired, is typically in the range of 30–40%. As a result, the scan duration is prolonged and depends heavily on the cardiac and respiratory rates.

As conventional LGE, HR-LGE acquisition is synchronized to patient's ECG. If PSIR reconstruction is compatible with 2-RR triggered HR-LGE,[35] 1-RR triggering is usually preferred not to double the scan time. Therefore, the inversion time of HR-LGE needs to be carefully chosen, due to the absence of PSIR reconstruction. However, the extended scan duration makes the inversion time more challenging to determine, as it continues to increase with gadolinium washout.[35] Consequently, the HR-LGE contrast may be suboptimal with a normal myocardium not perfectly nulled. For that reason, the most widely used strategy is to add an empirical offset to the inversion time (typically by adding 20–30 msec at 1.5 T and 50–80 msec at 3 T).[36–38] In the future, the development of PSIR techniques without the need for a reference image every other heartbeat may allow for HR-LGE with PSIR with the same acquisition time as HR-LGE without PSIR, and less sensitivity to the inversion time.[39,40]

The technical specifications of conventional LGE and HR-LGE sequences are summarized in Table 1.

Advantages and Limitations of HR-LGE

HR-LGE provides finer details and allows for a better characterization of the scar morphology. The clinical applications of such a high resolution will be covered in the related section of this review. Moreover, the free-breathing technique is particularly valuable for patients with poor compliance, for whom repeated breath-holds are cumbersome. Indeed, respiratory motion during conventional LGE leads to low-quality images with blurring and ghost artifacts.[6] Finally, clinicians can reconstruct any desired orientation of the HR-LGE whole-heart volume, using multiplanar reformatting,[31] while conventional LGE is limited to the prescribed long-axis and short-axis views.

Nonetheless, free-breathing HR-LGE suffers from several limitations. First, it is a time-consuming sequence, which may not be compatible with most clinical workflows. The average scan time is around 10 min ([min,max] = [5,16] minutes).[36–38,41,45–47] As a comparison, conventional breath-hold LGE lasts 5 min on average ([min,max] = [3,8] min) to complete the all views.[51] Second, HR-LGE acquisition may fail or be considered nondiagnostic: ~17% for atrial HR-LGE,[28] and ~8% (from 3% to 24%) for ventricular HR-LGE.[30,34,36,37,45,46,51] This discrepancy between atrial and ventricular HR-LGE may be explained by the thinness of the LA wall that can be more prone to blurring. The main reported causes are motion artifacts due to inconsistent breathing patterns, respiratory drift, low echo-navigator efficiency, arrhythmia or poor ECG-gating, bad contrast due to a poor inversion time, and claustrophobia. Conventional

TABLE 1. Technical Specifications of Conventional LGE and High-Resolution LGE Sequences

	Conventional LGE	HR-LGE
Sequence type	Inversion-recovery gradient-echo	
Spatial resolution	1.4–1.8 mm in plane 6–8 mm slice thickness with or without gap[3]	1.3–1.4 mm iso at 3 T[36,38,41–44] 1.5 × 1.5× 2.5 mm at 1.5 T[45–50]
Acquisition scheme	2D/3D	3D
Motion compensation technique	Breath-hold	Free-breathing with echo-navigator end-expiratory gating
Scan time mean [min max]	5 min [3 min – 8 min][51]	10 min[a] [5 min – 16 min][36–38,41,45–47]
Views	Repeated acquisition for each view	Whole-heart volume enabling reformatting in any view

[a]Average value from available data from references 36–38,41,45–47.
HR = high-resolution; LGE = late gadolinium enhancement.

LGE may also lead to nondiagnostic image quality due to poor breath-holding or arrhythmia, but compared to HR-LGE, acquisitions can be easily repeated with other strategies less prone to artifacts, such as single-shot with or without motion compensation.[33]

Quantitative Image Quality Comparison Between Conventional and HR-LGE in the Left Ventricle

Bizino et al demonstrated that increasing the LGE spatial resolution from $1.5 \times 1.5 \times 10$ mm^3 to $1.7 \times 1.7 \times 1.7$ mm^3 allows for improved sharpness and thus a better delineation of the scar.[37] Smaller, scattered lesions can be revealed by HR-LGE while conventional LGE would be negative.[35,47] It has been shown that the scar mass can be overestimated by conventional LGE.[35,37] The contrast-to-noise ratio between the myocardium and enhancement is decreased with HR-LGE, while the contrast between the lesions and LV blood pool is increased.[31,37] The latter could be explained by the longer delay between the injection and the acquisition of HR-LGE when compared with conventional LGE, resulting in a relatively larger wash-out of the gadolinium in the blood pool.

CLINICAL INDICATIONS FOR HR-LGE IMAGING ON THE ATRIA

Atrial fibrosis is a common pathophysiological factor to the onset and maintenance of atrial fibrillation (AFib) (Fig. 2). Over the last decade, HR-LGE imaging has allowed for a better understanding of the mechanisms involved in the pathophysiology of AFib.[52–54] Atrial HR-LGE has been proposed in several clinical indications: 1) to identify patients at risk for incident AFib, 2) to predict the risk of cardiovascular event in patients with AFib, 3) to predict postablation arrhythmia recurrence, 4) and to guide AFib ablation, and 5) to map postablation scar and guide repeat ablation procedures.

In patients without history of AFib, quantification of LA fibrosis using HR-LGE may identify patients at higher risk for incident AFib before the initiation of the arrhythmia. Indeed, significant differences in LA fibrosis extent have been described between patients without structural heart disease or AFib, patients with structural heart disease but without AFib, patients with paroxysmal AFib and patients with persistent AFib.[55] These results are in line with a recent study reporting significant extent of LA fibrosis in non-AFib patients highlighting that structural fibrosis may precede AFib onset.[56] Quail et al

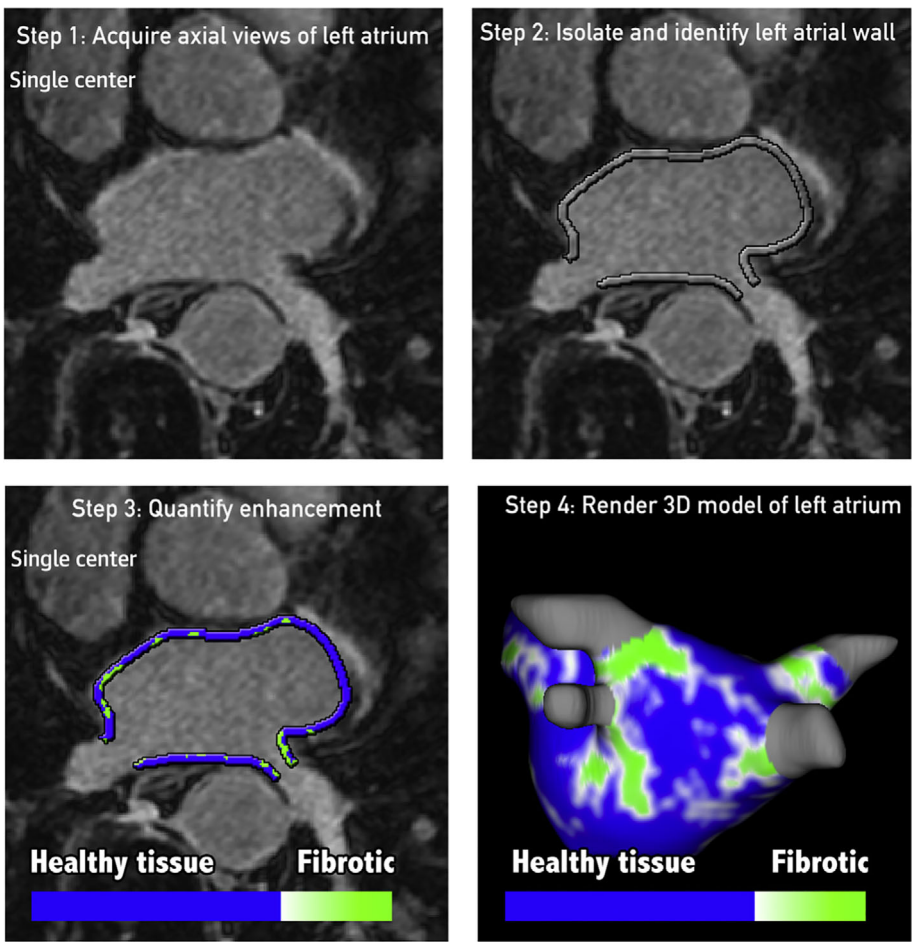

FIGURE 2: Atrial HR-LGE workflow. The following color coding is used: healthy tissue is depicted as blue, whereas any tissue with LGE is depicted as green. LGE = late gadolinium enhancement; MRI = magnetic resonance imaging. Reprinted from reference 28 with permission from Elsevier.

reported that a LA fibrosis extent >10% on HR-LGE was associated with an increase rate of new-onset AFib.[57]

Beyond predicting incident AFib, the quantification of LA fibrosis may play a prognostic role in patients already in AFib. Indeed, a study assessing 387 patients with AFib has shown that patients with previous ischemic stroke had a significantly higher extent of LA fibrosis.[58] Likewise, in a retrospective study of 1228 patients with AFib assessed by HR-LGE, a greater extent of LA fibrosis was associated with a higher occurrence of MACE, driven primarily by increased risk of stroke or transient ischemic attack.[59] Therefore, quantification of LA fibrosis could represent a helpful tool to stratify the risk of stroke additionally to the current clinical scores in patients with AFib.[60,61]

The analysis of LA fibrosis has also the potential to improve outcomes after AFib ablation procedures.[28] The DECAAF trial conducted across 15 clinical centers has shown that LA fibrosis quantified by HR-LGE was independently associated with recurrent arrhythmia after catheter ablation.[2] The authors introduced a staging approach (Utah classification) to assess the extent of LA fibrosis into four stages: stage 1 (<10% of the atrial wall), 2 (10%–20%), 3 (20%–30%), and 4 (≥30%).[2] The cumulative incidence of recurrent arrhythmia after 1 year was for stages 1–4: 15.3%, 32.6%, 45.9%, and 51.1%, respectively. This approach may allow for an improved selection of catheter ablation candidates, as patients in early Utah stages appear to have a more favorable LA structural and functional reverse remodeling, and higher long-term success.[62] In contrast, a conservative approach may be considered for patients with higher LA fibrosis burden assessed by CMR, due to the high risk of recurrent arrhythmia after catheter ablation.[63,64] In addition to patient selection, atrial fibrosis imaging may also play a role in improving the definition of catheter ablation targets. This aspect will soon be clarified by the ongoing DECAAF II trial, a randomized study comparing conventional AFib ablation (pulmonary vein isolation) with fibrosis-guided ablation (pulmonary vein isolation with additional targeting of CMR-defined fibrosis).[65]

In addition to atrial fibrosis imaging before catheter ablation, HR-LGE imaging has also been applied to the mapping and quantification of postablation scar. Postablation outcome was shown to be related to scar burden.[66] The approach can be valuable to assess the impact of novel ablation technologies on the atrial wall[67] and/or on adjacent structures potentially at risk for collateral damage such as the esophagus.[68,69] Some authors even suggested using HR-LGE to guide repeat ablation procedures on scar gaps as assessed by imaging.[70] This approach remains debated, because currently available CMR methods may not have sufficient spatial resolution to accurately describe the continuity of scar across the pulmonary vein circumference and throughout the transmurality of the thin atrial wall.[67,71]

It is important to note however that despite promising research results, atrial fibrosis imaging has not yet lived up to its full clinical potential. After a decade of research, atrial LGE is still not part of recommended imaging protocols and patient management algorithms in patients with AFib. Indeed, the method is still hampered by a limited availability, a suboptimal feasibility (particularly in patients scanned in AFib), and by the insufficient reproducibility and lack of standard for robust LGE quantification on the atria (see dedicated section below).[72]

VENTRICULAR HIGH-RESOLUTION LATE GADOLINIUM ENHANCEMENT

HR-LGE offers an improved spatial resolution at the expense of an extended acquisition time, which does not make it compatible with most clinical workflows. In the LV, conventional LGE remains the established gold standard, and HR-LGE should be added to traditional routine for specific patients who would benefit the most from it. In this section, we detail the applications in which ventricular HR-LGE showed a clinical value (Table 2). An illustration of the interest of ventricular HR-LGE is shown in patients in Fig. 3 in direct comparison with conventional LGE.

Ventricular Arrhythmia

DETECTION OF THE VENTRICULAR ARRHYTHMOGENIC SUBSTRATE. In patients with ventricular arrhythmias, focal scar detection may have a direct impact on therapeutic decision, potentially leading to the introduction of antiarrhythmic drugs or specific recommendations for exercise practice. HR-LGE allows for the detection of the arrhythmogenic substrate at a higher spatial resolution. In a study investigating 157 patients with ventricular arrhythmia, HR-LGE was shown to significantly improve the diagnostic yield of CMR,[45] allowing for the detection of small nontransmural scars undetected with conventional LGE, associated with the diagnosis of nonischemic cardiomyopathy in 70% of patients, ischemic cardiomyopathy in 20%, and arrhythmogenic right ventricular cardiomyopathy (ARVC) in 10%. In all cases, electroanatomical mapping (EAM) confirmed that the detected scars were the origin of the arrhythmia. The addition of HR-LGE was particularly useful in patients with no prior history of structural heart disease and with negative findings on echocardiography, coronary angiography, and conventional CMR methods.

Of note, this study showed that HR-LGE can be instrumental in confirming the diagnosis of ARVC, by revealing RV LGE co-localized with borderline wall motion abnormalities on cine images (Fig. 4). In the current Task Force recommendations, LGE is not part of the ARVC diagnostic criteria.[73] Indeed, RV LGE cannot be reliably detected by

TABLE 2. Clinical Studies Based on HR-LGE Acquisitions

References	Year	Patient Group	Magnetic Field Strength	HR-LGE Spatial Resolution (mm)	Acquisition Time	Failure of HR-LGE Acquisition	Main Findings
48	2013	Nine patients referred for VT ablation: three ICM, three NICM, two myocarditis, and one idiopathic VT, including 7 (78%) with HR-LGE	1.5 T	1.25 × 1.25 × 2.5	NA	0 patients	Feasibility of integration of HR-LGE in EAM system for the guidance of VT ablation, with an excellent match between low-voltages maps and HR-LGE in patients with ICM and myocarditis.
36	2013	21 patients with remote MI submitted for VT ablation	3 T	1.4 iso	Mean ± SD: 16 ± 8 min	Two patients for low-quality images	HR-LGE identified 74% of the critical isthmus of clinical VT, and 50% of all the conducting channels.
41	2014	15 patients with repaired tetralogy of Fallot	3 T	1.3 iso	Mean ± SD: 7 min 6 s ± 2 min 30 s	One patient with severe motion-related artifact due to coughing	Feasibility, accuracy and reproducibility of HR-LGE imaging in repaired tetralogy of Fallot.
50	2015	12 patients referred for postmyocarditis VT ablation, including 7 (58%) with HR-LGE	1.5 T	1.25 × 1.25 × 2.5	NA	NA	HR-LGE is useful before ablation to precisely identify the location of epicardial scar, as epicardial mapping is limited by epicardial fat.
38	2015	30 patients referred for VT ablation: 23 ICM, and 7 NICM	3 T	1.4 iso	Mean ± SD: 16 min 26 s ± 7 min 32 s	One patient with claustrophobia	HR-LGE improves conducting channels delineation prior to VT ablation compared to conventional LGE, with EAM as gold standard.
49	2016	116 referred for catheter ablation, including 35 (30%) with HR-LGE	1.5 T	1.25 × 1.25 × 2.5	NA	NA	Feasibility of HR-LGE guided VT ablation with a positive impact on procedural management. The image integration influenced the decision to add voltage mapping measurements in abnormal HR-LGE areas and the decision to undertake an epicardial approach.

TABLE 2. Continued

References	Year	Patient Group	Magnetic Field Strength	HR-LGE Spatial Resolution (mm)	Acquisition Time	Failure of HR-LGE Acquisition	Main Findings
43	2016	90 patients referred for post-MI VT ablation, including 41 (46%) with HR-LGE	3 T	1.4 iso	NA	NA	Image-based strategy decision for VT ablation in post-MI patients (epicardial vs. endo-epicardial) provides a lower VT-recurrence rate.
45	2017	157 patients referred for ventricular arrhythmia management	1.5 T	1.25 × 1.25 × 2.5	5–10 min	NA	HR-LGE changes the final diagnosis in 13% of patients.
44	2017	159 patients referred for VT ablation, including 54 (34%) with HR-LGE to guide ablation	3 T	1.4 iso	NA	NA	HR-LGE guided VT ablation was associated with: • a lower need for radiofrequency delivery, • a higher non-inducibility rate after ablation, • and a lower VT-recurrence rate.
42	2018	217 patients referred for cardiac resynchronization therapy, including 73 (34%) with HR-LGE	3 T	1.4 iso	NA	NA	The presence, extension, heterogeneity, and qualitative distribution of border zones were independently associated with appropriate implantable-cardioverter-defibrillator therapies and sudden cardiac death.
46	2019	101 patients with repaired tetralogy of Fallot, including 75 (73%) patients with HR-LGE	1.5 T	1.25 × 1.25 × 2.5	5–10 min	NA	Scar size quantified by HR-LGE was independently associated with ventricular arrhythmia.
47	2020	229 MINOCA patients, including 172 (75%) with HR-LGE	1.5 T	1.25 × 1.25 × 2.5	8–12 min	Five patients due to poor tolerance during CMR	HR-LGE changed the final diagnosis in 26% of patients.

In all these clinical studies, the HR-LGE sequence was an ECG-triggered inversion-recovery gradient echo sequence with a diaphragmatic echo-navigator.
CMR = cardiovascular magnetic resonance; EAM = electroanatomical mapping; ECG = electrocardiogram; HR = high-resolution; ICM = ischemic cardiomyopathy, iso = isotropic; LGE = late gadolinium enhancement; MI = myocardial infarction; MINOCA = myocardial infarction with nonobstructive coronary arteries; NA = not available; NICM = nonischemic cardiomyopathy; SD = standard deviation; VT = ventricular tachycardia.

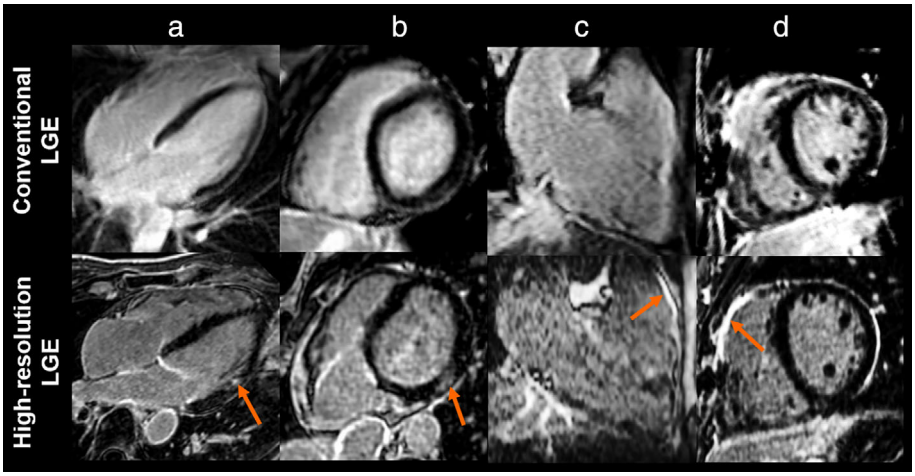

FIGURE 3: Late gadolinium enhancement (LGE) images from conventional LGE (top row) and high-resolution LGE (bottom row) in patients with myocardial infarction defined by sub-endocardial LGE (a), myocarditis with sub-epicardial LGE (b), arrhythmogenic right ventricular cardiomyopathy (c), and repaired tetralogy of Fallot with LGE at the surgical scar (d) (for all, LGE is designated by the yellow arrows). These images are adapted from references 11,12,16 with the courtesy of Prof. Cochet.

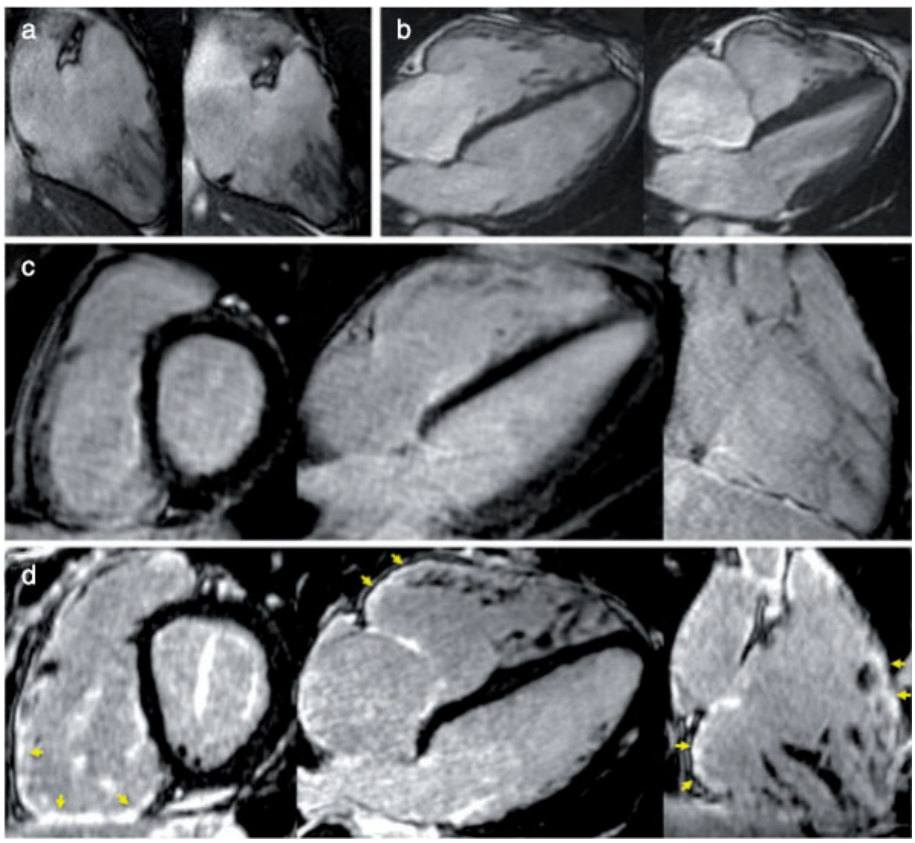

FIGURE 4: Example of ARVC diagnosis using HR-LGE sequence. A 20-year-old man with family history of premature sudden death in the brother. Cine images showed preserved RV ejection fraction, mild RV dilatation, and borderline wall motion abnormality (a and b). Conventional LGE images were considered normal (c). HR-LGE showed focal fibrosis on infero-basal and laterobasal RV as well as on RV outflow track (arrows in d). The colocalization between fibrosis and the suspected wall motion abnormality was instrumental in retaining a minor Task Force Criterion for ARVC, fulfilling the criteria for definite ARVC diagnosis. ARVC = arrhythmogenic right ventricular cardiomyopathy; LGE = late gadolinium enhancement; HR = high resolution. Reprinted from reference 45 with permission from Oxford University Press.

conventional LGE.[74,75] However, due to its higher resolution, HR-LGE may become an important adjunct tool to cine imaging, potentially improving reader confidence in the complex interpretation of RV regional wall motion abnormalities. Further studies with larger samples are necessary to confirm these observations.

CHARACTERIZATION OF MYOCARDIAL SCAR HETEROGENEITY AND RISK STRATIFICATION OF CARDIOVASCULAR EVENTS. Myocardial scar can be heterogeneous with surviving bundles of myocytes mixed with fibrotic tissue, and this specific tissue is the substrate on which reentrant ventricular tachycardia (VT) can develop. This "border zone," also called "grey zone," can be identified by LGE, based on its intermediate signal intensity as compared to the dense hypersignal of the scar core. The border zone comprises both the "peri-infarct zone," that is, the transition between dense scar tissues and the surrounding healthy tissue at the scar periphery, and the "conducting channels," that is, corridors of viable tissue penetrating within the scar. The quantification of the grey zone by conventional LGE has been shown to predict long-term mortality, the inducibility of ventricular arrhythmia and appropriate implantable cardioverter-defibrillator therapy defined as the occurrence of anti-tachycardia pacing or shocks delivered for VT.[76–78] These findings have been very recently confirmed in a larger cohort of 979 patients with coronary artery disease for the prediction of sudden cardiac death.[79] In this study, a grey zone >5 g was superior to left ventricular ejection fraction <35% to predict sudden cardiac death.

The smaller voxels of HR-LGE offer a better characterization of the scar complexity by reducing the partial volume effect and the strong voxel anisotropy.[80] Indeed, Dzyubachyk et al demonstrated in postinfarction patients that conventional LGE overestimated grey zones compared to an interpolated HR-LGE volume, with EAM as gold standard.[81] Furthermore, HR-LGE allows the reconstruction of complex 3D scar architecture using dedicated software. A color-coded representation of the different types of tissue (normal, scar core and border zone) is provided at different depths inside the ventricular walls (Fig. 5).[82] HR-LGE was compared to EAM as a gold standard, to confirm its ability to identify the arrhythmogenic substrate, and to define the best cutoff value in LGE signal intensity to distinguish border zones from the scar core. In some preliminary studies, 70–81% of EAM conducting channels could be identified on HR-LGE, using a spatial resolution of $1.4 \times 1.4 \times 1.4\ mm^3$ at 3 T.[36,38,83] A good agreement was also found at 1.5 T between low voltage areas and HR-LGE with a spatial resolution of $1.25 \times 1.25 \times 2.5\ mm^3$.[48] Finally, HR-LGE was shown to identify more conducting channels in correlation with EAM than conventional LGE,[38] emphasizing the need for a high spatial resolution to well characterize the scar geometry and quantify the border zones.

Recently, HR-LGE ($1.5 \times 1.5 \times 1.5\ mm^3$) was used in infarct animal model to highlight the limitations of EAM at identifying scar.[84] Indeed, voltage maps only reflect tissue characteristics within few millimeters at the vicinity of the catheter tip, limiting its sensitivity to detect mid-myocardial scar. In particular, EAM mismatched with HR-LGE in preserved wall thickness with extended scar from subendocardial to epicardium regions. This discordance advocates the use of HR-LGE in combination with EAM in patients undergoing VT ablation.

The presence, extension, heterogeneity, and distribution of border zones were independent predictors of an additional risk of life-threatening ventricular arrhythmia and sudden cardiac death in 217 patients with cardiac resynchronization therapy, over a follow-up period of 3 years.[42] This study suggested that the conducting channels were more closely related to arrhythmic events than peri-infarct zones. These

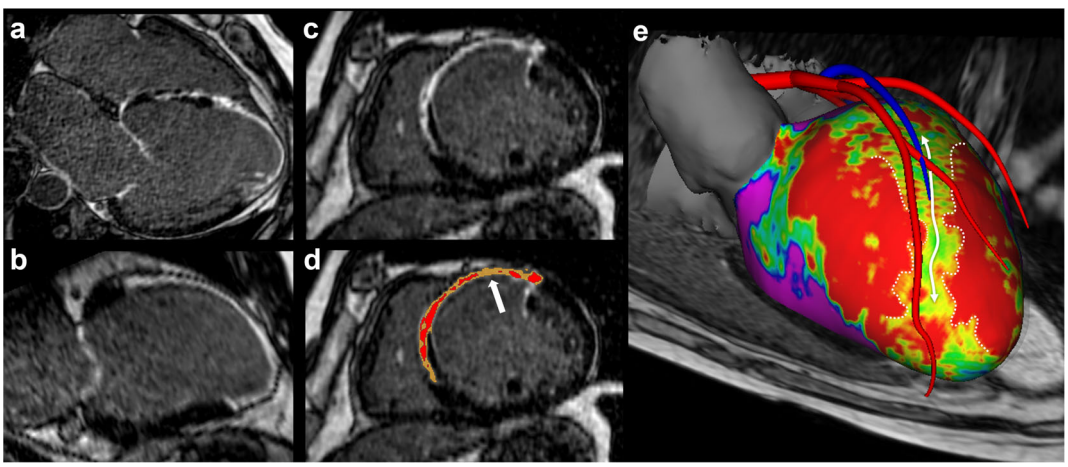

FIGURE 5: Detection of arrhythmogenic sites within post-infarction scar using HR-LGE. The transversal acquisition volume can be reformatted in any orientation (a: 4-chamber, b: 2-chamber, c: short axis). Intensity signal analysis can distinguish the grey zone (d, yellow) from dense scar (d, red). In order to guide the catheter ablation of ventricular tachycardia, the HR-LGE dataset can be segmented to generate a patient-specific 3D model displaying myocardial scar geometry and heterogeneity embedded within a highly detailed cardiac anatomy (e, anterior view). The color-coded map shows scar density at 20% transmurality (purple: remote myocardium, green to yellow: grey zone, red: dense scar). A channel of grey zone penetrating a dense scar can be seen in the anteroseptal area (d and e, white arrows). HR-LGE = high-resolution late gadolinium enhancement.

TABLE 3. Studies Assessing the Feasibility of Accelerated Implementations of HR-LGE

Reference	Patients Year group	Magnetic Field strength	HR-LGE Spatial resolution	Field of View (mm)	Motion Compensation Technique	Acceleration Technique	HR-LGE Acquisition Time	Failure or Low-Quality HR-LGE Acquisition	Main Findings
102	2012 14 patients	1.5 T	1.7 mm iso	320 × 320 × 120	Diaphragmatic echo-navigator	Compressed sensing (with LOST technique), factor 3	NA	One patient	Feasibility of HR-LGE imaging using compressed-sensing to enable high isotropic spatial resolution.
103	2016 16 patients	1.5 T	1.2 mm iso	220 × 220 × 220	Self-navigation[a]: extraction of the breathing signal in the imaging data.	3D radial with spiral phyllotaxis pattern, factor	8.2 min ± 0.9 min	Two patients due to striking artifacts	Feasibility of self-navigated radial HR-LGE with improved sharpness compared to conventional LGE.
104	2017 270 patients	1.5 T	1.5 × 1.5 × 3 mm	320 × 320 × 100–120 mm	Diaphragmatic echo-navigator	Compressed sensing (with LOST technique), factor 3 or 5	6.4 min with factor 3, and 4 min with factor 5	NA	Feasibility of HR-LGE with compressed-sensing acceleration (excellent image quality in >80% patients) with similar diagnostic performance to conventional LGE.
105	2017 23 patients	1.5 T	2 mm iso (recon. 1 mm iso)	320 × 320 × 120	iNAV[b]	Parallel imaging, factor 2	3.9 min ± 1.65 min	One patient due to fast arrhythmia	Feasibility of iNAV HR-LGE with similar diagnostic performance to conventional LGE.
106	2017 12 patients	1.5 T	1 × 1 × 4 mm (recon. 1 × 1 × 2 mm)	320 × 320 × 80–130 mm	iNAV[b]	Cartesian trajectory with spiral profile	12.1 min ± 1.9 min	One patient	Feasibility of simultaneous bright-blood coronary angiography and black blood HR-LGE.

TABLE 3. Continued

Reference	Patients Year group	Magnetic Field strength	HR-LGE Spatial resolution	Field of View (mm)	Motion Compensation Technique	Acceleration Technique	HR-LGE Acquisition Time	Failure or Low-Quality HR-LGE Acquisition	Main Findings
107	2020 15 patients	1.5 T	1.3 mm iso	312 × 312 × 83–114 mm	iNAV[b]	Compressed-sensing (with HD-PROST reconstruction technique), factor 3	8 min ± 1.4 min	Two patients due to magnetic field inhomogeneities and residual cardiac motion with poor myocardial nulling	Feasibility of water/fat HR-LGE with iNAV.
108	2020 40 patients	1.5 T	1.3 mm iso	312 × 312 × 83–114 mm	iNAV[b]	Compressed-sensing (with HD-PROST reconstruction technique), factor 2.6	10.8 min	None	Similar LGE detection compared to conventional LGE, and superior evaluation of pericarditis due to better fat suppression using DIXON.
109	2020 70 patients	1.5 T	1.4 mm iso	298 × 265 × 120 mm	Diaphragmatic echo-navigator	Compressed SENSE, factor 5	4.5 min ± 1.4 min	Seven patients with poor image quality	Good image quality of HR-LGE in 80% of patients in shorter scan time than conventional LGE, with an improved depiction of small lesions
110	2021 78 patients	1.5 T	1.8 mm iso	300 × 300 × 135 mm	Diaphragmatic echo-navigator	Compressed SENSE, factor 9	3.5 min	19 patients with poor image quality	Higher confidence in diagnosis of subepicardial LGE due to improved fat suppression using DIXON compared to conventional LGE

[a]Self-navigation: respiratory-induced heart motion is directly obtained from the imaging data itself without any echo-navigator.
[b]iNAV: The 1D diaphragmatic echo-navigator is replaced by a 2D image-based navigator that can directly track the motion of the heart. 100% of the breathing cycle is used for acquisition to accelerate the HR-LGE acquisition. The motion is then compensated with a nonrigid algorithm during the image reconstruction, to ensure a good image quality without motion artifacts.
HD-PROST = high-dimensionality undersampled patch-based reconstruction; HR-LGE = high-resolution late gadolinium enhancement; iNAV = image-based navigator; iso = isotropic; LOST = low-dimensional-structure self-learning and threshold; NA = not available; recon = reconstructed.

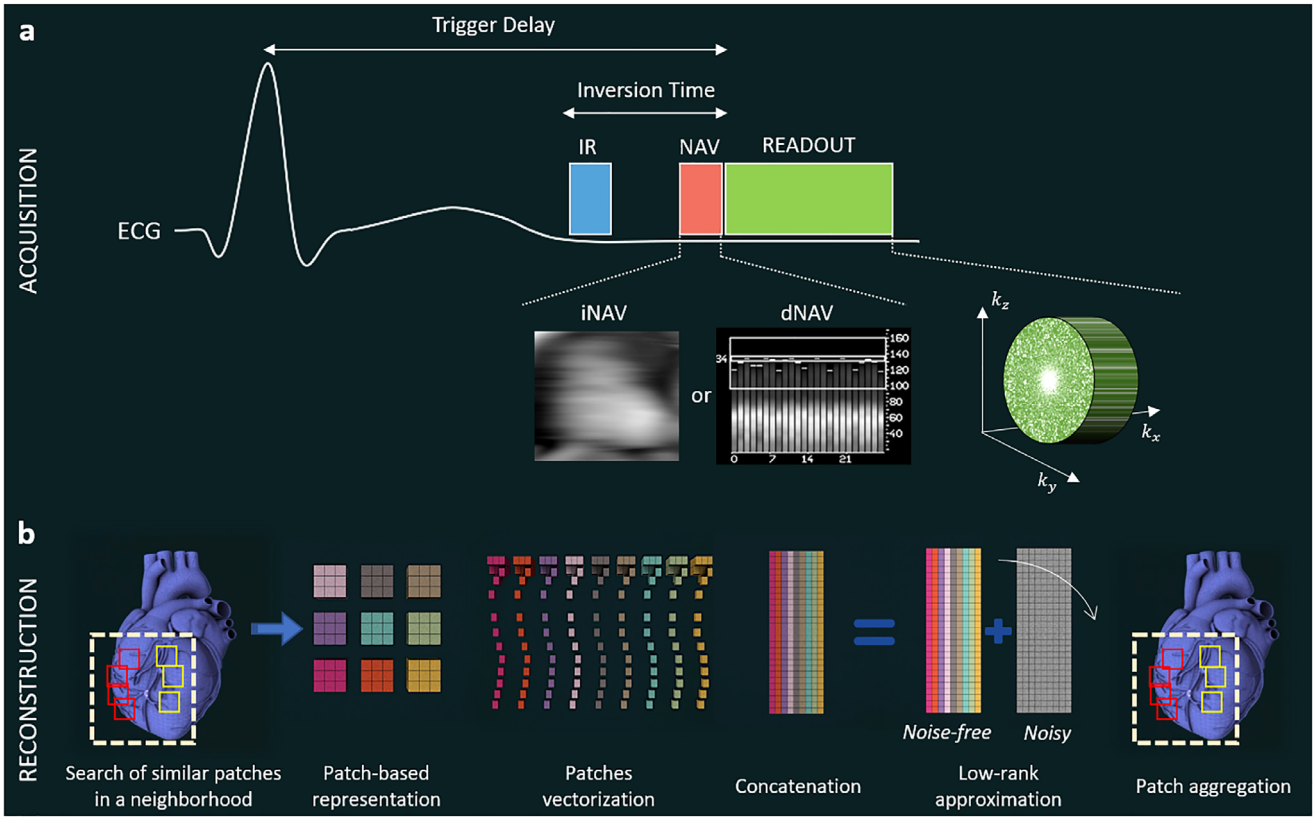

FIGURE 6: Acquisition and reconstruction concepts for accelerated whole-heart HR-LGE. (a) Acquisition is performed using an inversion pulse to null the healthy-myocardium signal, an echo-navigator to track and correct the respiratory motion of the heart and an undersampled variable-density Poisson-like 3D trajectory to accelerate the scan time. (b) For image reconstruction, similar patches in the image are first selected, vectorized and concatenated in a matrix. This matrix, being low-rank in a mathematical sense, can be decomposed into a noisy matrix and a clean matrix using a high-order tensor decomposition (HD-PROST) or a 3D fast Fourier transform (LOST) with a shrinkage of the coefficients. Only the clean matrix is kept, and denoised patches are placed back in their original position via patch aggregation. These steps are repeated for all patches in the image, and a denoised 3D volume is eventually obtained. IR = inversion recovery; iNAV = image-based navigator; dNAV = diaphragmatic-based navigator.

results highlight the potential of HR-LGE to improve myocardial scar tissue characterization, and thus the risk stratification of cardiovascular events.

VENTRICULAR TACHYCARDIA ABLATION GUIDANCE. Substrate-based VT ablation relies on the elimination of excitable conducting channels to block VT circuits. The identification of the substrate is usually performed via point-by-point voltage mapping, which can be time-consuming and hampered by low resolution or low catheter/wall contact. The integration of HR-LGE images into EAM navigation systems to guide substrate-based VT ablation is feasible and compatible with clinical practice[48,49,83] (Fig. 5), producing a direct impact on procedural management. Indeed, HR-LGE has been shown to improve the localization of the target ablation sites and motivates the electrophysiologist to perform additional mapping points.[48,49] Furthermore, the detailed scar location influences the ablation strategy and the optimal approach: endocardial, epicardial, or combined. This is of particular value in patients with transmural MI or subepicardial postmyocarditis scar,[43,50] in whom epicardial or combined approaches may be considered. The impact of HR-LGE integration was assessed in a prospective nonrandomized study of 159 patients undergoing VT ablation, in which 54 patients had HR-LGE image integration.[44] This study reported the use of HR-LGE minimized the number of radiofrequency applications and radiofrequency delivery time and was associated with a higher rate of acute success, defined as noninducibility of any sustained VT at the end of the procedure. Consequently, the HR-LGE group had a lower ventricular arrhythmia recurrence rate than the control group over a mean follow-up of 1.7 ± 1.6 years, suggesting a more complete ablation of the arrhythmogenic substrate. In a subset of patients, some conducting channels only identified with HR-LGE and not with EAM were not ablated. These patients had a higher recurrence rate of VT at follow-up, suggesting that HR-LGE could identify an arrhythmogenic substrate not visible with EAM. These promising findings need to be confirmed by a prospective randomized study.

Congenital Heart Disease

The lifespan of adults with adult congenital heart disease (ACHD) has dramatically improved with advances in

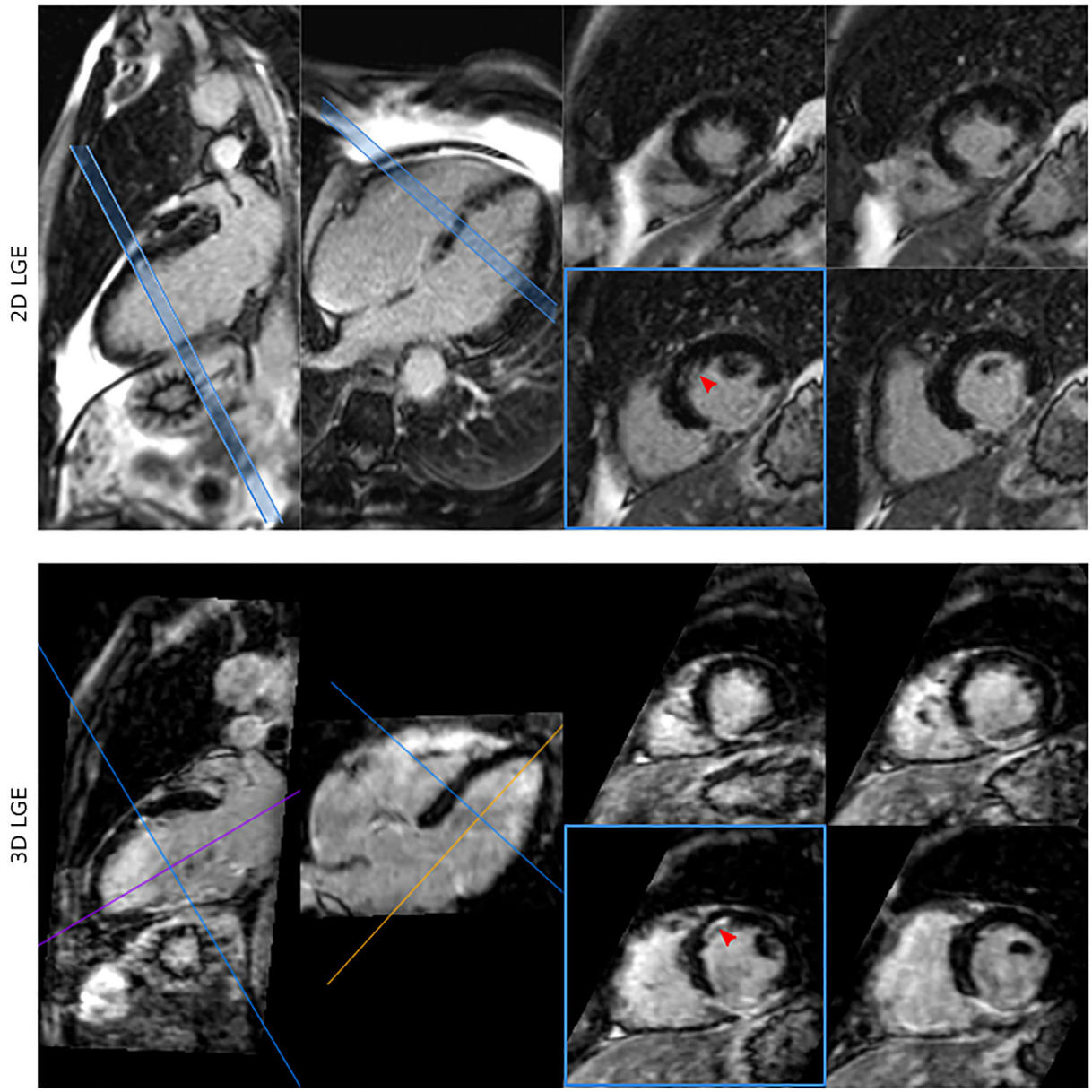

FIGURE 7: Whole-heart HR-LGE with fat-water separation. Visual comparison between conventional LGE and HR-LGE images showing small subendocardial infarction that can be observed in the mid-anterior wall (red arrow) in both sets of images, with a better depiction in the long axis in the case of the conventional LGE images; and a good depiction in both long and short axis views in the 3D HR-LGE images. Reprinted from reference 107 with permission from BMC.

cardiac surgery. In 2010, this population was estimated to be 1.4 million in the United States.[85] The management and imaging of these patients may be challenging because of the heterogeneity of ACHD, the complexity of anatomical abnormalities, pre- and post-surgery, and long-term complications, such as heart failure, arrhythmia and associated sudden cardiac death.[86] The risk stratification of these patients is difficult due to a poorly understood disease progression. Complex ACHD examples include tetralogy of Fallot (TOF), transposition of the great arteries, Ebstein's anomaly, and single ventricle congenital heart disease. In these diseases, myocardial fibrosis is a common finding in surgical sites, as expected, but also in remote locations such as the RV.[87] LGE imaging is crucial to assess the prognosis and tailor therapy.[88] The use of conventional LGE leads to frequent false positives in the thin-walled RV, in which voxels may be contaminated by epicardial fat.[88] In this context, HR-LGE has been successfully used to characterize surgical scarring and fibrosis in patients with repaired TOF.[41,46] Interestingly, the HR-LGE focal scar size has been shown to correlate with biventricular systolic dysfunction and ventricular arrhythmia.[46] This technique may help identify applications to better characterize the arrhythmogenic substrate and guide the ablation procedure, as previously described.

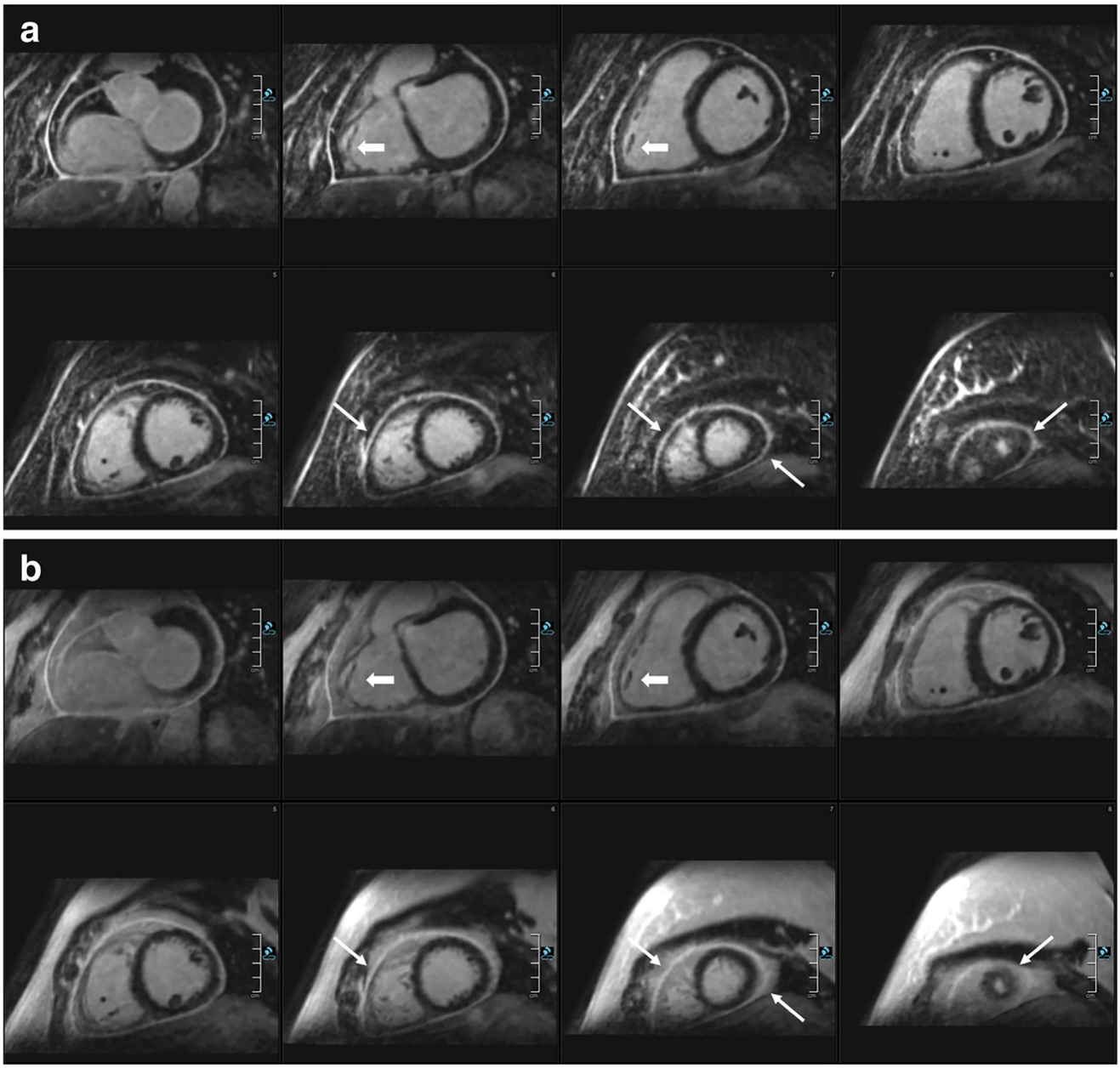

FIGURE 8: Comparison of (a) HR-LGE with fat-water separation (DIXON) and (b) conventional 2D LGE in a female patient with pericarditis. DIXON-based fat suppression enables excellent delimitation of the enhanced pericardium against the epicardial fat. In direct comparison, the pericardium can hardly be identified in several areas in the HR-LGE views and worse in the conventional LGE views (thin arrows: eg, along the right ventricle, close to the apex). Moreover, 3D water LGE imaging allows for excellent depiction of small details such as the trabeculae of the right ventricle (bold arrows). Reprinted from reference 108 with permission from Springer.

Myocardial Infarction With Nonobstructed Coronary Arteries

Identifying the underlying etiology of MINOCA is a major challenge in clinical practice. CMR plays a pivotal role in distinguishing patients with actual MI from patients with nonischemic causes of acute coronary syndrome (myocarditis, Takotsubo, and other cardiomyopathies).[89] However, in 21%–26% of patients, CMR is normal or inconclusive, leading to a management dilemma.[89,90] Lintingre et al very recently investigated the diagnostic value of adding HR-LGE to the CMR protocol in 172 patients with MINOCA, when conventional LGE was inconclusive (i.e., negative or compatible with several diagnoses).[47] Interestingly, HR-LGE led to a change in final diagnosis in 26% of the patients. In two-thirds of these patients, the diagnostic change occurred when conventional LGE was compatible with several diagnoses. The remaining patients had small myocardial lesions in the LV and RV only revealed via HR-LGE while conventional LGE was negative. This study highlights the fact that small myocardial injuries may be missed by conventional LGE, due

to a lack of spatial resolution.[35] Detecting LGE has major implications for the therapeutic management of patients with MINOCA, advocating for the use of the HR-LGE sequence when conventional LGE is negative or uncertain.

HR-LGE SEGMENTATION AND QUANTIFICATION

Quantitative measurements of conventional LGE are usually based on signal intensity thresholding of a manually segmented region of interest (ROI) of the myocardial borders.[91] The two main approaches are the n-SD technique (with $n = 2, 3, 4, 5, 6\ldots$) and the "full width half maximum" (FWHM) technique. They both rely on the manual outlining of endocardial and epicardial borders. In the n-SD technique, a threshold between normal myocardium is determined above the standard deviation (SD) of the manually selected remote (dark) myocardium.[92] There is no established cut-off, but 5-SD is recommended for myocardial infarction as a starting point before manual adjustment.[91] In the FWHM technique, half the maximal signal within the scar is the threshold between normal myocardium and LGE.[76,80] However, these two strategies rely on the manual segmentation of myocardial borders, which are subject to high inter- and intra-observer variability.[93] The lack of consistency and the labor-intensive nature of these techniques hinder their wide adoption in clinical routine. Nowadays, conventional LGE extent is visually assessed using American Heart Association 17-segment model[94] along with the transmurality (0%, 1–25%, 26–50%, 51–75% and 76–100%). Multiple methods for quantifying the extent of grey zones have been reported: between 35% and –50% of maximal LGE intensity using the FWHM technique,[77] or signal intensity above the maximal intensity of the remote myocardium,[76,80] or finally between 2-SD and 3-SD of remote myocardium intensity.[95] Recently, the technique between 2-SD and 3-SD was shown to be the most associated with sudden cardiac death in patients with coronary artery disease, compared to FWHM method.[79] However, due to the strong impact of partial volume effect with conventional LGE, the 2020 SCMR Task Force on Standardized Post-Processing does not support any specific evaluation technique.[81,91]

An accurate segmentation of whole-heart HR-LGE is one the key aspect of CMR-guided ablation procedures in the LA and the ventricles. Indeed, as already mentioned, HR-LGE was first initially developed to better visualize and quantify LA fibrosis to guide AFib ablation. However, LA fibrosis segmentation is particularly challenging due to the thin atrial wall nearby surrounding structures such as the aortic wall and valves. The majority of the centers participating to DECAAF study used manual or semimanual segmentation with thresholds adjusted by an expert operator (usually >2-SD or >4-SD above the mean signal intensity of the normal myocardium).[1,28] Another approach consisted in normalizing the intensity of the LA wall by the mean value of the blood pool signal.[96] However, there is no agreement on what threshold value should be used to identify fibrosis. The discrepancy of LA fibrosis segmentation methods between groups may be explained by patient-specific factors (anatomy, contrast clearance rate, heterogeneity of the myocardial scar) and by factors impacting HR-LGE images (field strength, spatial resolution, signal-to-noise ratio, inversion time, artifacts, etc).

Segmentation of left ventricular LGE is also crucial for image integration in EAM systems for VT ablation guidance. Segmentation of scar core, grey zones, and normal myocardium in the left ventricle usually relies on a fixed threshold relative to the peak LGE intensity (FWHM technique). Fernandez et al classified voxels >60% of maximal intensity as scar core, and 40%–60% as grey zone,[36] while Cochet et al used >50% and 35%–50% for scar core and grey zone, respectively.[48] This discrepancy can be explained by different field strength (3 T vs. 1.5 T, respectively), spatial resolution ($1.4 \times 1.4 \times 1.4$ mm^3 vs. $1.25 \times 1.25 \times 2.5$ mm^3, respectively) among other factors influencing HR-LGE signal intensities.

Overall, the segmentation of HR-LGE either for LA or LV fibrosis is a time-consuming, tedious, and error-prone process with limited robustness and reproducibility. In addition, the use of thresholding methods relies on a user-dependent delineation of myocardial borders and there is no consensus on threshold cutoff values. To alleviate the burden of HR-LGE segmentation, artificial intelligence, particularly deep learning, will undoubtedly provide alternative solutions to automate this task and improve accuracy and reproducibility. To this regard, benchmarking of algorithms is crucial to evaluate how novel segmentation methods perform relative to other existing state-of-the-art algorithms. The "Left Atrium Segmentation Challenge" was organized during the 2018 MICCAI conference using 154 HR-LGE annotated datasets. A remarkable Dice accuracy score of 93.2% was achieved using the most popular conventional neural networks (CNN) architecture in medical imaging segmentation, the U-net, significantly outperforming state-of-the-art algorithms.[97–99] Particularly, a two-stage 3D CNN method was employed to 1) crop the HR-LGE volume to address the severe class imbalance between the under-represented LA and the over-represented background noise and 2) to locally segment the targeted area. To ensure further clinical deployment, larger multi-center datasets should be built to encounter for multiple scanner vendors and the variability of HR-LGE image quality. Contrary to atrial HR-LGE, no benchmarking or "challenge" have been implemented yet for ventricular HR-LGE, as it already exists with conventional LGE.[72] However, the feasibility of fully automated segmentation has been demonstrated by Kurzendorfer et al who achieved a Dice accuracy

score of ~80% on 30 HR-LGE datasets from two centers using texture-based analysis.[100] More recently, using a training dataset of only 34 HR-LGE, a deep learning approach was developed using several U-Nets and yielded Dice score of 83%.[101]

In the future, the clinical availability of such fully automated algorithms for HR-LGE segmentation will enrich the robustness and reproducibility of LA and LV fibrosis quantification. The implications are not only for MR-guided ablation procedures but also for cardiovascular events risk stratification. Indeed, LA fibrosis and LV grey zones are associated with adverse outcomes, and their precise quantification allowed by HR-LGE, would be helpful to personalize patient management.[59,77,79]

FUTURE DEVELOPMENTS OF HR-LGE

The long HR-LGE scan duration limits its wide clinical adoption. Technical progress has been made to accelerate HR-LGE 1) by acquiring less data using innovative acquisition techniques and 2) by improving the respiratory motion compensation efficiency (Table 3).

Acquisition and Reconstruction Strategies

The feasibility of accelerated HR-LGE has been demonstrated by acquiring fewer k-space samples and exploiting their compressibility using compressed-sensing approaches[102,111–114] (Fig. 6). Advanced undersampling strategies have to be considered and such state-of-the-art techniques often rely on pseudo-random Cartesian trajectories such as variable-density Poisson-like samplings.[102,104,107] In order to recover images with good image quality from undersampled acquisitions, iterative reconstruction frameworks have been based on exploiting the similarity of small local patches in the 3D images through low-rank decomposition to increase SNR and reduce undersampling artifacts. These reconstruction tools, known as LOST for single-contrast CMR[102] and HD-PROST for multicontrast CMR,[115] have shown promising results in being able to increase the spatial resolution and accelerate the scan time of free-breathing whole-heart images. Basha et al assessed the clinical feasibility of this strategy on 270 patients ($1.4 \times 1.4 \times 1.4$ mm^3, 5-fold acceleration, ~4 min scan time) and concluded that an acceptable image quality could be achieved in most patients.[104]

Recently, Pennig et al combined regular compressed sensing technique with parallel imaging to accelerate HR-LGE ($1.4 \times 1.4 \times 1.4$ mm^3, 5-fold acceleration, 4 min 30 sec average scan time) and achieved a good to excellent image quality in 80% of patients with decreased overall scan time as compared to conventional LGE.[109] Direct comparison between HR-LGE and conventional LGE showed an improved depiction of small and particularly nonischemic lesions, further confirming the usefulness of HR-LGE.

Respiratory Motion Compensation

The diaphragmatic echo-navigator imposes a long and unpredictable scan time, as only 30–40% of the heartbeats are used. Moreover, irregular breathing patterns may worsen the navigator efficiency to less than 10%, leading to non-diagnostic images or acquisition failure. Novel developments have been recently introduced to allow for 100% efficiency (no rejected data) and thus, a predictable and reduced scan time.[116] The diaphragmatic echo-navigator is replaced by a more sophisticated 2D image-based echo-navigator (iNAV) that directly tracks the heart motion and allows for more complex motion compensation, such as non-rigid motion. The feasibility of 3D iNAV HR-LGE has been recently demonstrated with a similar image quality to conventional LGE in 22 patients, with a reduced scan time of 4 min.[105] Another strategy is to detect heart motion directly from the imaging data itself without any echo-navigator.[103] Self-navigated HR-LGE was successfully used in patients with a radial acquisition of $1.15 \times 1.15 \times 1.15$ mm^3 isotropic resolution, producing improved image sharpness compared to conventional LGE. However, the self-navigated HR-LGE acquisition lasts around 8 min and has a risk of streaking artifacts. Non-Cartesian stack-of-radial HR-LGE was also reported without the need of motion compensation and thus a significant scan time reduction (<3 min with $1.25 \times 1.25 \times 2.5$ mm^3 spatial resolution).[114] However, the evaluation was limited to five patients and further studies are needed to confirm the diagnostic performance of such approach.

Similarly to developments in conventional LGE, advances in HR-LGE contrast have also been developed, such as black-blood HR-LGE with simultaneous whole-heart coronary angiography,[106] and wide-band HR-LGE to reduce the artifacts caused by implantable devices.[117] DIXON HR-LGE has also been proposed recently to improve the suppression of the epicardial fat (Fig. 7).[107,108,110] This new approach improved the confidence in diagnosis of subepicardial LGE compared to conventional 3D single breath-hold LGE.[110] DIXON fat suppression may also improve the evaluation of the extent of pericardial involvement by HR-LGE in patients suspected with pericarditis (Fig. 8).[108] The diagnostic performance of all these advanced techniques in clinical routine needs to be assessed in further studies.

CONCLUSIONS

Over the last decade, the technical development of HR-LGE imaging has allowed for accurate identification and efficient quantification of LA fibrosis. The clinical applications of LA fibrosis imaging are numerous and steadily increasing, ranging from early identification of patients at risk of incident AFib to prediction of the risk of stroke or arrhythmia recurrence in patients with AFib, for guiding the catheter ablation. However, while this MR sequence was initially developed to

characterize LA fibrosis, it presents a significant interest in the ventricles as well. As compared to conventional LGE, ventricular HR-LGE imaging appears to be a valuable tool that could significantly impact decision-making in clinical routine. Indeed, the use of HR-LGE can lead to diagnostic changes, based on the detection of small scars, which are nonvisible with conventional LGE. This proved to be particularly helpful in patients with MINOCA or ventricular arrhythmia of an unknown etiology when the conventional LGE is negative or inconclusive. In addition, 3D HR-LGE images can now be integrated in EAM systems to guide ablations, producing a direct impact on procedure management. Based on detailed scar visualization, a need for an epicardial approach can be anticipated, and the targeted tissue can be more accurately identified. Initial results suggesting a decrease in VT-recurrence due to more complete ablations with HR-LGE need to be confirmed by randomized studies. Finally, the RV fibrosis visualization by HR-LGE might be of great interest to improve the clinician confidence in the challenging diagnosis of ARVC and to better characterize patients with ACHD, such as a repaired tetralogy of Fallot. Considering the extended scan time of ventricular HR-LGE, the challenge is to select the patients who would benefit the most from it. Future studies will be needed to explore the previously mentioned indications of ventricular HR-LGE. Regarding the left atrial HR-LGE, the ongoing DECAAF II trial will help define the best technical approach to catheter ablation of persistent AFib and precise the selection criteria for ablation. The new technical developments currently made to accelerate HR-LGE are promising for a more widespread use of this sequence.

Acknowledgments

The research leading to these results has received funding from l'Agence Nationale de la Recherche (ANR) under Grant Agreements Equipex MUSIC ANR-11-EQPX-0030 and LIRYC ANR-10-IAHU-04, and the European Research Council under Grant Agreement ERC n°715093.

Conflict of Interest

The authors declare that the research was conducted in the absence of any commercial or financial relationship that could be construed as a potential conflict of interest.

References

1. Oakes RS, Badger TJ, Kholmovski EG, et al. Detection and quantification of left atrial structural remodeling with delayed-enhancement magnetic resonance imaging in patients with atrial fibrillation. Circulation 2009;119:1758-1767.
2. Marrouche NF, Wilber D, Hindricks G, et al. Association of atrial tissue fibrosis Identified by delayed enhancement MRI and atrial fibrillation catheter ablation: The DECAAF study. Jama 2014;311:498.
3. Kramer CM, Barkhausen J, Bucciarelli-Ducci C, Flamm SD, Kim RJ, Nagel E. Standardized cardiovascular magnetic resonance imaging (CMR) protocols: 2020 update. J Cardiovasc Magn Reson 2020;22:17.
4. Kawel N, Turkbey EB, Carr JJ, et al. Normal left ventricular myocardial thickness for middle-aged and older subjects with steady-state free precession cardiac magnetic resonance: The multi-ethnic study of atherosclerosis. Circ Cardiovasc Imaging 2012;5:500-508.
5. Peters DC, Wylie JV, Hauser TH, et al. Detection of pulmonary vein and left atrial scar after catheter ablation with three-dimensional navigator-gated delayed enhancement MR imaging: Initial experience[1]. Radiology 2007;243:690-695.
6. Kellman P, Arai AE. Cardiac imaging techniques for physicians: Late enhancement. J Magn Reson Imaging 2012;36:529-542.
7. Goetti R, Kozerke S, Donati OF, et al. Acute, subacute, and chronic myocardial infarction: Quantitative comparison of 2D and 3D late gadolinium enhancement MR imaging. Radiology 2011;259:704-711.
8. Morita K, Utsunomiya D, Oda S, et al. Comparison of 3D phase-sensitive inversion-recovery and 2D inversion-recovery MRI at 3.0 T for the assessment of late gadolinium enhancement in patients with hypertrophic cardiomyopathy. Acad Radiol 2013;20:752-757.
9. Morsbach F, Gordic S, Gruner C, et al. Quantitative comparison of 2D and 3D late gadolinium enhancement MR imaging in patients with Fabry disease and hypertrophic cardiomyopathy. Int J Cardiol 2016; 217:167-173.
10. Polacin M, Kapos I, Gastl M, et al. Comparison of 3D and 2D late gadolinium enhancement magnetic resonance imaging in patients with acute and chronic myocarditis. Int J Cardiovasc Imaging 2021;37: 305-313.
11. Bratis K, Henningsson M, Grigoratos C, et al. Clinical evaluation of three-dimensional late enhancement MRI: Clinical evaluation of 3D-LGE. J Magn Reson Imaging 2017;45:1675-1683.
12. Kellman P, Arai AE, McVeigh ER, Aletras AH. Phase-sensitive inversion recovery for detecting myocardial infarction using gadolinium-delayed hyperenhancement. Magn Reson Med 2002;47:372-383.
13. Liu C-Y, Wieben O, Brittain JH, Reeder SB. Improved delayed enhanced myocardial imaging with T_2 -prep inversion recovery magnetization preparation. J Magn Reson Imaging 2008;28:1280-1286.
14. Muscogiuri G, Rehwald WG, Schoepf UJ, et al. T(rho) and magnetization transfer and INvErsion recovery (TRAMINER)-prepared imaging: A novel contrast-enhanced flow-independent dark-blood technique for the evaluation of myocardial late gadolinium enhancement in patients with myocardial infarction: Dark blood MRI for myocardial LGE. J Magn Reson Imaging 2017;45:1429-1437.
15. Kim HW, Rehwald WG, Jenista ER, et al. Dark-blood delayed enhancement cardiac magnetic resonance of myocardial infarction. JACC Cardiovasc Imaging 2018;11:1758-1769.
16. Basha T, Roujol S, Kissinger KV, Goddu B, Manning WJ, Nezafat R. Black blood late gadolinium enhancement using combined T2 magnetization preparation and inversion recovery. J Cardiovasc Magn Reson 2015;17:O14.
17. Basha TA, Tang MC, Tsao C, et al. Improved dark blood late gadolinium enhancement (DB-LGE) imaging using an optimized joint inversion preparation and T_2 magnetization preparation: Improved DB-LGE using joint inversion and T_2 magnetization prep. Magn Reson Med 2018;79:351-360.
18. Kellman P, Xue H, Olivieri LJ, et al. Dark blood late enhancement imaging. J Cardiovasc Magn Reson 2017;18:77.
19. Fahmy AS, Neisius U, Tsao CW, et al. Gray blood late gadolinium enhancement cardiovascular magnetic resonance for improved detection of myocardial scar. J Cardiovasc Magn Reson 2018;20:22.
20. Francis R, Kellman P, Kotecha T, et al. Prospective comparison of novel dark blood late gadolinium enhancement with conventional bright blood imaging for the detection of scar. J Cardiovasc Magn Reson 2017;19:91.
21. Holtackers RJ, Chiribiri A, Schneider T, Higgins DM, Botnar RM. Dark-blood late gadolinium enhancement without additional magnetization preparation. J Cardiovasc Magn Reson 2017;19:64.

22. Vermes E, Carbone I, Friedrich MG, Merchant N. Patterns of myocardial late enhancement: Typical and atypical features. Arch Cardiovasc Dis 2012;105:300-308.

23. Bière L, Piriou N, Ernande L, Rouzet F, Lairez O. Imaging of myocarditis and inflammatory cardiomyopathies. Arch Cardiovasc Dis 2019; 112:630-641.

24. Latus H, Gummel K, Klingel K, et al. Focal myocardial fibrosis assessed by late gadolinium enhancement cardiovascular magnetic resonance in children and adolescents with dilated cardiomyopathy. J Cardiovasc Magn Reson 2015;17:34.

25. Ederhy S, Mansencal N, Réant P, Piriou N, Barone-Rochette G. Role of multimodality imaging in the diagnosis and management of cardiomyopathies. Arch Cardiovasc Dis 2019;112:615-629.

26. Wong TC, Piehler K, Puntil KS, et al. Effectiveness of late gadolinium enhancement to improve outcomes prediction in patients referred for cardiovascular magnetic resonance after echocardiography. J Cardiovasc Magn Reson 2013;15:6.

27. Kuruvilla S, Adenaw N, Katwal AB, Lipinski MJ, Kramer CM, Salerno M. Late gadolinium enhancement on cardiac magnetic resonance predicts adverse cardiovascular outcomes in nonischemic cardiomyopathy: A systematic review and meta-analysis. Circ Cardiovasc Imaging 2014;7:250-258.

28. Siebermair J, Kholmovski EG, Marrouche N. Assessment of left atrial fibrosis by late gadolinium enhancement magnetic resonance imaging. JACC Clin Electrophysiol 2017;3:791-802.

29. Kellman P, Larson AC, Hsu L-Y, et al. Motion-corrected free-breathing delayed enhancement imaging of myocardial infarction. Magn Reson Med 2005;53:194-200.

30. Ledesma-Carbayo MJ, Kellman P, Arai AE, McVeigh ER. Motion corrected free-breathing delayed-enhancement imaging of myocardial infarction using nonrigid registration. J Magn Reson Imaging 2007;26:184-190.

31. Amano Y, Matsumura Y, Kumita S. Free-breathing high-spatial-resolution delayed contrast-enhanced three-dimensional viability MR imaging of the myocardium at 3.0T: A feasibility study. J Magn Reson Imaging 2008;28:1361-1367.

32. Nguyen TD, Spincemaille P, Weinsaft JW, et al. A fast navigator-gated 3D sequence for delayed enhancement MRI of the myocardium: Comparison with breathhold 2D imaging. J Magn Reson Imaging 2008;27: 802-808.

33. Piehler KM, Wong TC, Puntil KS, et al. Free-breathing, motion-corrected late gadolinium enhancement is robust and extends risk stratification to vulnerable patients. Circ Cardiovasc Imaging 2013;6: 423-432.

34. Olivieri L, Cross R, O'Brien KJ, Xue H, Kellman P, Hansen MS. Free-breathing motion-corrected late-gadolinium-enhancement imaging improves image quality in children. Pediatr Radiol 2016;46:983-990.

35. Kino A, Zuehlsdorff S, Sheehan JJ, et al. Three-dimensional phase-sensitive inversion-recovery turbo FLASH sequence for the evaluation of left ventricular myocardial scar. Am J Roentgenol 2009;193:W381-W388.

36. Fernández-Armenta J, Berruezo A, Andreu D, et al. Three-dimensional architecture of scar and conducting channels based on high resolution ce-CMR: Insights for ventricular tachycardia ablation. Circ Arrhythm Electrophysiol 2013;6:528-537.

37. Bizino MB, Tao Q, Amersfoort J, et al. High spatial resolution free-breathing 3D late gadolinium enhancement cardiac magnetic resonance imaging in ischaemic and non-ischaemic cardiomyopathy: Quantitative assessment of scar mass and image quality. Eur Radiol 2018;28:4027-4035.

38. Andreu D, Ortiz-Pérez JT, Fernández-Armenta J, et al. 3D delayed-enhanced magnetic resonance sequences improve conducting channel delineation prior to ventricular tachycardia ablation. EP Eur 2015; 17:938-945.

39. Wang J, Chen H, Maki JH, et al. Referenceless Acquisition of Phase-sensitive Inversion-recovery with decisive reconstruction (RAPID) imaging: RAPID imaging. Magn Reson Med 2014;72:806-815.

40. Liu H, Wilson GJ, Balu N, et al. 3D true-phase polarity recovery with independent phase estimation using three-tier stacks based region growing (3D-TRIPS). Magn Reson Mater Phys Biol Med 2018;31: 87-99.

41. Stirrat J, Rajchl M, Bergin L, Patton DJ, Peters T, White JA. High-resolution 3-dimensional late gadolinium enhancement scar imaging in surgically corrected tetralogy of Fallot: Clinical feasibility of volumetric quantification and visualization. J Cardiovasc Magn Reson 2014;16:76.

42. Acosta J, Fernández-Armenta J, Borràs R, et al. Scar characterization to predict life-threatening arrhythmic events and sudden cardiac death in patients with cardiac resynchronization therapy. JACC Cardiovasc Imaging 2018;11:561-572.

43. Acosta J, Fernández-Armenta J, Penela D, et al. Infarct transmurality as a criterion for first-line endo-epicardial substrate–guided ventricular tachycardia ablation in ischemic cardiomyopathy. Heart Rhythm 2016; 13:85-95.

44. Andreu D, Penela D, Acosta J, et al. Cardiac magnetic resonance–aided scar dechanneling: Influence on acute and long-term outcomes. Heart Rhythm 2017;14:1121-1128.

45. Hennig A, Salel M, Sacher F, et al. High-resolution three-dimensional late gadolinium-enhanced cardiac magnetic resonance imaging to identify the underlying substrate of ventricular arrhythmia. EP Eur 2018;20:f179-f191.

46. Cochet H, Iriart X, Allain-Nicolaï A, et al. Focal scar and diffuse myocardial fibrosis are independent imaging markers in repaired tetralogy of Fallot. Eur Heart J - Cardiovasc Imaging 2019;20:990-1003.

47. Lintingre P-F, Nivet H, Clément-Guinaudeau S, et al. High-resolution late gadolinium enhancement magnetic resonance for the diagnosis of myocardial infarction with nonobstructed coronary arteries. JACC Cardiovasc Imaging 2020;13:1135-1148.

48. Cochet H, Komatsu Y, Sacher F, et al. Integration of merged delayed-enhanced magnetic resonance imaging and multidetector computed tomography for the guidance of ventricular tachycardia ablation: A pilot study. J Cardiovasc Electrophysiol 2013;24:419-426.

49. Yamashita S, Sacher F, Mahida S, et al. Image integration to guide catheter ablation in scar-related ventricular tachycardia: Image integration-guided VT ablation. J Cardiovasc Electrophysiol 2016;27: 699-708.

50. Berte B, Sacher F, Cochet H, et al. Postmyocarditis ventricular tachycardia in patients with epicardial-only scar: A specific entity requiring a specific approach: Epicardial-only VT ablation. J Cardiovasc Electrophysiol 2015;26:42-50.

51. Muehlberg F, Arnhold K, Fritschi S, et al. Comparison of fast multislice and standard segmented techniques for detection of late gadolinium enhancement in ischemic and non-ischemic cardiomyopathy – A prospective clinical cardiovascular magnetic resonance trial. J Cardiovasc Magn Reson 2018;20:13.

52. Spragg D. Left atrial fibrosis: Role in atrial fibrillation pathophysiology and treatment outcomes. J Atr Fibrillation 2013;5:810.

53. Gal P, Marrouche NF. Magnetic resonance imaging of atrial fibrosis: Redefining atrial fibrillation to a syndrome. Eur Heart J 2017;38:14-19.

54. Burstein B, Nattel S. Atrial fibrosis: Mechanisms and clinical relevance in atrial fibrillation. J Am Coll Cardiol 2008;51:802-809.

55. Cochet H, Mouries A, Nivet H, et al. Age, atrial fibrillation, and structural heart disease are the Main determinants of left atrial fibrosis detected by delayed-enhanced magnetic resonance imaging in a general cardiology population: Atrial fibrosis on MRI in patients. J Cardiovasc Electrophysiol 2015;26:484-492.

56. Siebermair J, Suksaranjit P, McGann CJ, et al. Atrial fibrosis in non–atrial fibrillation individuals and prediction of atrial fibrillation by use of late gadolinium enhancement magnetic resonance imaging. J Cardiovasc Electrophysiol 2019;30:550-556.

57. Quail M, Grunseich K, Baldassarre LA, et al. Prognostic and functional implications of left atrial late gadolinium enhancement cardiovascular magnetic resonance. J Cardiovasc Magn Reson 2019;21:2.

58. Daccarett M, Badger TJ, Akoum N, et al. Association of left atrial fibrosis detected by delayed-enhancement magnetic resonance imaging and the risk of stroke in patients with atrial fibrillation. J Am Coll Cardiol 2011;57:831-838.

59. King JB, Azadani PN, Suksaranjit P, et al. Left atrial fibrosis and risk of cerebrovascular and cardiovascular events in patients with atrial fibrillation. J Am Coll Cardiol 2017;70:1311-1321.

60. Olesen J, Torp-Pedersen C, Hansen M, Lip G. The value of the CHA2DS2-VASc score for refining stroke risk stratification in patients with atrial fibrillation with a CHADS2 score 0–1: A nationwide cohort study. Thromb Haemost 2012;107:1172-1179.

61. Hindricks G, Potpara T, Dagres N, et al. 2020 ESC guidelines for the diagnosis and management of atrial fibrillation developed in collaboration with the European Association for Cardio-Thoracic Surgery (EACTS). Eur Heart J 2021;42:373-498.

62. Kuppahally SS, Akoum N, Badger TJ, et al. Echocardiographic left atrial reverse remodeling after catheter ablation of atrial fibrillation is predicted by preablation delayed enhancement of left atrium by magnetic resonance imaging. Am Heart J 2010;160:877-884.

63. Akoum N, Fernandez G, Wilson B, Mcgann C, Kholmovski E, Marrouche N. Association of atrial fibrosis quantified using LGE-MRI with atrial appendage thrombus and spontaneous contrast on transesophageal echocardiography in patients with atrial fibrillation: Atrial fibrosis and appendage thrombus. J Cardiovasc Electrophysiol 2013; 24:1104-1109.

64. Akoum N, Daccarett M, Mcgann C, et al. Atrial fibrosis helps select the appropriate patient and strategy in catheter ablation of atrial fibrillation: A DE-MRI guided approach. J Cardiovasc Electrophysiol 2011; 22:16-22.

65. Marrouche NF, Greene T, Dean JM, et al. Efficacy of LGE-MRI-guided fibrosis ablation versus conventional catheter ablation of atrial fibrillation: The DECAAF II trial: Study design. J Cardiovasc Electrophysiol 2021;32(4):916-924.

66. Akoum N, Wilber D, Hindricks G, et al. MRI assessment of ablation-induced scarring in atrial fibrillation: Analysis from the DECAAF study: MRI assessment of ablation-induced scarring in atrial fibrillation. J Cardiovasc Electrophysiol 2015;26:473-480.

67. Jefairi NA, Camaioni C, Sridi S, et al. Relationship between atrial scar on cardiac magnetic resonance and pulmonary vein reconnection after catheter ablation for paroxysmal atrial fibrillation. J Cardiovasc Electrophysiol 2019;30:727-740.

68. Badger TJ, Adjei-Poku YA, Burgon NS, et al. Initial experience of assessing esophageal tissue injury and recovery using delayed-enhancement MRI after atrial fibrillation ablation. Circ Arrhythm Electrophysiol 2009;2:620-625.

69. Baher A, Kheirkhahan M, Rechenmacher SJ, et al. High-power radiofrequency catheter ablation of atrial fibrillation: Using late gadolinium enhancement magnetic resonance imaging as a novel index of esophageal injury. JACC Clin Electrophysiol 2018;4:1583-1594.

70. Bisbal F, Guiu E, Cabanas-Grandío P, et al. CMR-guided approach to localize and ablate gaps in repeat AF ablation procedure. JACC Cardiovasc Imaging 2014;7:653-663.

71. Harrison JL, Sohns C, Linton NW, et al. Repeat left atrial catheter ablation: Cardiac magnetic resonance prediction of endocardial voltage and gaps in ablation lesion sets. Circ Arrhythm Electrophysiol 2015;8: 270-278.

72. Karim R, Bhagirath P, Claus P, et al. Evaluation of state-of-the-art segmentation algorithms for left ventricle infarct from late gadolinium enhancement MR images. Med Image Anal 2016;30:95-107.

73. Marcus FI, McKenna WJ, Sherrill D, et al. Diagnosis of arrhythmogenic right ventricular cardiomyopathy/dysplasia: Proposed modification of the task force criteria. Circulation 2010;121:1533-1541.

74. te Riele AS, Tandri H, Bluemke DA. Arrhythmogenic right ventricular cardiomyopathy (ARVC): Cardiovascular magnetic resonance update. J Cardiovasc Magn Reson 2014;16:50.

75. Selton-Suty C, Juillière Y. Non-invasive investigations of the right heart: How and why? Arch Cardiovasc Dis 2009;102:219-232.

76. Schmidt A, Azevedo CF, Cheng A, et al. Infarct tissue heterogeneity by magnetic resonance imaging identifies enhanced cardiac arrhythmia susceptibility in patients with left ventricular dysfunction. Circulation 2007;115:2006-2014.

77. Haghbayan H, Lougheed N, Deva DP, Chan KKW, Lima JAC, Yan AT. Peri-infarct quantification by cardiac magnetic resonance to predict outcomes in ischemic cardiomyopathy: Prognostic systematic review and meta-analysis. Circ Cardiovasc Imaging 2019;12:e009156.

78. Rayatzadeh H, Tan A, Chan RH, et al. Scar heterogeneity on cardiovascular magnetic resonance as a predictor of appropriate implantable cardioverter defibrillator therapy. J Cardiovasc Magn Reson 2013;15:31.

79. Zegard A, Okafor O, de Bono J, et al. Myocardial fibrosis as a predictor of sudden death in patients with coronary artery disease. J Am Coll Cardiol 2021;77:29-41.

80. Peters DC, Appelbaum EA, Nezafat R, et al. Left ventricular infarct size, peri-infarct zone, and papillary scar measurements: A comparison of high-resolution 3D and conventional 2D late gadolinium enhancement cardiac MR. J Magn Reson Imaging 2009;30:794-800.

81. Dzyubachyk O, Tao Q, Poot DHJ, et al. Super-resolution reconstruction of late gadolinium-enhanced MRI for improved myocardial scar assessment: SRR for late gadolinium-enhanced MRI. J Magn Reson Imaging 2015;42:160-167.

82. Mukherjee RK, Whitaker J, Williams SE, Razavi R, O'Neill MD. Magnetic resonance imaging guidance for the optimization of ventricular tachycardia ablation. EP Eur 2018;20:1721-1732.

83. Andreu D, Berruezo A, Ortiz-Pérez JT, et al. Integration of 3D electroanatomic maps and magnetic resonance scar characterization into the navigation system to guide ventricular tachycardia ablation. Circ Arrhythm Electrophysiol 2011;4:674-683.

84. Kucukseymen S, Yavin H, Barkagan M, et al. Discordance in scar detection between electroanatomical mapping and cardiac MRI in an infarct swine model. JACC Clin Electrophysiol 2020;6:1452-1464.

85. Gilboa SM, Devine OJ, Kucik JE, et al. Congenital heart defects in the United States: Estimating the magnitude of the affected population in 2010. Circulation 2016;134:101-109.

86. Endorsed by the Association for European Paediatric Cardiology (AEPC), Authors/Task Force Members, Baumgartner H, et al. ESC guidelines for the management of grown-up congenital heart disease (new version 2010): The task force on the Management of Grown-up Congenital Heart Disease of the European Society of Cardiology (ESC). Eur Heart J 2010;31:2915-2957.

87. Bonello B, Kilner PJ. Review of the role of cardiovascular magnetic resonance in congenital heart disease, with a focus on right ventricle assessment. Arch Cardiovasc Dis 2012;105:605-613.

88. Ghonim S, Voges I, Gatehouse PD, et al. Myocardial architecture, mechanics, and fibrosis in congenital heart disease. Front Cardiovasc Med 2017;4:30.

89. Pasupathy S, Air T, Dreyer RP, Tavella R, Beltrame JF. Systematic review of patients presenting with suspected myocardial infarction and nonobstructive coronary arteries. Circulation 2015;131:861-870.

90. Dastidar AG, Baritussio A, De Garate E, et al. Prognostic role of CMR and conventional risk factors in myocardial infarction with nonobstructed coronary arteries. JACC Cardiovasc Imaging 2019;12: 1973-1982.

91. Schulz-Menger J, Bluemke DA, Bremerich J, et al. Standardized image interpretation and post-processing in cardiovascular magnetic resonance - 2020 update: Society for Cardiovascular Magnetic Resonance (SCMR): Board of Trustees Task Force on standardized post-processing. J Cardiovasc Magn Reson 2020;22:19.

92. Kolipaka A, Chatzimavroudis GP, White RD, O'Donnell TP, Setser RM. Segmentation of non-viable myocardium in delayed enhancement magnetic resonance images. Int J Cardiovasc Imaging 2005;21: 303-311.

93. Klem I, Heiberg E, Van Assche L, et al. Sources of variability in quantification of cardiovascular magnetic resonance infarct size - reproducibility among three core laboratories. J Cardiovasc Magn Reson 2017; 19:62.

94. American Heart Association Writing Group on Myocardial Segmentation and Registration for Cardiac Imaging, Cerqueira MD, Weissman NJ, et al. Standardized myocardial segmentation and nomenclature for tomographic imaging of the heart: A statement for healthcare professionals from the cardiac imaging Committee of the Council on clinical cardiology of the American Heart Association. Circulation 2002;105:539-542.

95. Yan AT, Shayne AJ, Brown KA, et al. Characterization of the Peri-infarct zone by contrast-enhanced cardiac magnetic resonance imaging is a powerful predictor of post–myocardial infarction mortality. Circulation 2006;114:32-39.

96. Khurram IM, Beinart R, Zipunnikov V, et al. Magnetic resonance image intensity ratio, a normalized measure to enable interpatient comparability of left atrial fibrosis. Heart Rhythm 2014;11:85-92.

97. Pop M, Sermesant M, Zhao J, et al., editors. *Statistical Atlases and Computational Models of the Heart. Atrial Segmentation and LV Quantification Challenges: 9th International Workshop, STACOM 2018, Held in Conjunction with MICCAI 2018, Granada, Spain, September 16, 2018, Revised Selected Papers. Volume 11395*. Cham: Springer International Publishing; 2019.

98. Jamart K, Xiong Z, Maso Talou GD, Stiles MK, Zhao J. Mini review: Deep learning for atrial segmentation from late gadolinium-enhanced MRIs. Front Cardiovasc Med 2020;7:86.

99. Xiong Z, Xia Q, Hu Z, et al. A global benchmark of algorithms for segmenting the left atrium from late gadolinium-enhanced cardiac magnetic resonance imaging. Med Image Anal 2021;67:101832.

100. Kurzendorfer T, Forman C, Schmidt M, Tillmanns C, Maier A, Brost A. Fully automatic segmentation of left ventricular anatomy in 3-D LGE-MRI. Comput Med Imaging Graph 2017;59:13-27.

101. Zabihollahy F, Rajchl M, White JA, Ukwatta E. Fully automated segmentation of left ventricular scar from 3D late gadolinium enhancement magnetic resonance imaging using a cascaded multi-planar U-net (CMPU-net). Med Phys 2020;47:1645-1655.

102. Akçakaya M, Rayatzadeh H, Basha TA, et al. Accelerated late gadolinium enhancement cardiac MR imaging with isotropic spatial resolution using compressed sensing: Initial experience. Radiology 2012;264: 691-699.

103. Rutz T, Piccini D, Coppo S, et al. Improved border sharpness of post-infarct scar by a novel self-navigated free-breathing high-resolution 3D whole-heart inversion recovery magnetic resonance approach. Int J Cardiovasc Imaging 2016;32:1735-1744.

104. Basha TA, Akçakaya M, Liew C, et al. Clinical performance of high-resolution late gadolinium enhancement imaging with compressed sensing: High-resolution LGE with compressed sensing. J Magn Reson Imaging 2017;46:1829-1838.

105. Bratis K, Henningsson M, Grigoratos C, et al. Image-navigated 3-dimensional late gadolinium enhancement cardiovascular magnetic resonance imaging: Feasibility and initial clinical results. J Cardiovasc Magn Reson 2017;19:97.

106. Ginami G, Neji R, Rashid I, et al. 3D whole-heart phase sensitive inversion recovery CMR for simultaneous black-blood late gadolinium enhancement and bright-blood coronary CMR angiography. J Cardiovasc Magn Reson 2017;19:94.

107. Munoz C, Bustin A, Neji R, et al. Motion-corrected 3D whole-heart water-fat high-resolution late gadolinium enhancement cardiovascular magnetic resonance imaging. J Cardiovasc Magn Reson 2020;22:53.

108. Zeilinger MG, Wiesmüller M, Forman C, et al. 3D Dixon water-fat LGE imaging with image navigator and compressed sensing in cardiac MRI. Eur Radiol 2020;31:3951-3961.

109. Pennig L, Lennartz S, Wagner A, et al. Clinical application of free-breathing 3D whole heart late gadolinium enhancement cardiovascular magnetic resonance with high isotropic spatial resolution using compressed SENSE. J Cardiovasc Magn Reson 2020;22:89.

110. Dessouky R, De Stasio V, Boccalini S, et al. Comparison of free breathing 3D mDIXON with single breath-hold 3D inversion recovery sequences for the assessment of late gadolinium enhancement. Eur J Radiol 2021;134:109427.

111. Roujol S, Basha TA, Akçakaya M, et al. 3D late gadolinium enhancement in a single prolonged breath-hold using supplemental oxygenation and hyperventilation: Breath-hold 3D late gadolinium enhancement imaging. Magn Reson Med 2014;72:850-857.

112. Zhang L, Athavale P, Pop M, Wright GA. Multicontrast reconstruction using compressed sensing with low rank and spatially varying edge-preserving constraints for high-resolution MR characterization of myocardial infarction: High-resolution myocardial tissue characterization. Magn Reson Med 2017;78:598-610.

113. Kamesh Iyer S, Tasdizen T, Burgon N, et al. Compressed sensing for rapid late gadolinium enhanced imaging of the left atrium: A preliminary study. Magn Reson Imaging 2016;34:846-854.

114. Adluru G, Chen L, Kim S-E, et al. Three-dimensional late gadolinium enhancement imaging of the left atrium with a hybrid radial acquisition and compressed sensing. J Magn Reson Imaging 2011;34:1465-1471.

115. Bustin A, Lima da Cruz G, Jaubert O, Lopez K, Botnar RM, Prieto C. High-dimensionality undersampled patch-based reconstruction (HD-PROST) for accelerated multi-contrast MRI. Magn Reson Med 2019; 81:3705-3719.

116. Henningsson M, Koken P, Stehning C, Razavi R, Prieto C, Botnar RM. Whole-heart coronary MR angiography with 2D self-navigated image reconstruction. Magn Reson Med 2012;67:437-445.

117. Rashid S, Rapacchi S, Shivkumar K, Plotnik A, Finn JP, Hu P. Modified wideband three-dimensional late gadolinium enhancement MRI for patients with implantable cardiac devices: 3D LGE MRI for patients with ICDs. Magn Reson Med 2016;75:572-584.